Atmospheric Sounding Data as Tools for Forecasting Severe Hail and Ozone Accumulation in Arizona during the North American Monsoon

by

Jonny William Malloy

A Dissertation Presented in Partial Fulfillment
of the Requirements for the Degree
Doctor of Philosophy

Approved March 2019 by the
Graduate Supervisory Committee

Randall S. Cerveny, Chair
Nancy J. Selover
Anthony J. Brazel
Robert C. Balling Jr.

ARIZONA STATE UNIVERSITY

May 2019

ABSTRACT

Monsoon hazards routinely affect the community, economy, and environment of the American Southwest. A common link for hazard development during the North American Monsoon concerns the interplay between temperature, moisture, and wind in the vertical atmosphere controlled by an unstable monsoon circulation. This dissertation investigates vertical atmospheric patterns using in-situ sounding data, specifically, 1) environments favorable for severe hail on the Colorado Plateau, 2) significant parameters distinguishing unhealthy versus healthy ozone days in Phoenix, Arizona, and 3) vertical profile alignments associated with distinct ranges in ozone concentrations observed in Phoenix having defined health impacts.

The first study (published in the *Journal of the Arizona-Nevada Academy of Science*) determines significant variables on Flagstaff, Arizona 12Z rawinsonde data (1996-2009) found on severe hail days on the Colorado Plateau. Severe hail is related to greater sub-300 hectopascals (hPa) moisture, a warmer atmospheric column, lighter above surface wind speeds, more southerly to southeasterly oriented winds throughout the vertical (except at the 700 hPa pressure level), and higher geopotential heights.

The second study (published in *Atmospheric Environment*) employs principal component, linear discriminant, and synoptic composite analyses using Phoenix, Arizona rawinsonde data (2006-2016) to identify common monsoon patterns affecting ozone accumulation in the Phoenix metropolitan area. Unhealthy ozone occurs with amplified high-pressure ridging over the Four Corners region, 500 hPa heights often exceeding 5910 meters, surface afternoon temperatures typically over 40°C, lighter wind speeds in

the planetary boundary layer under four ms^{-1}, and persistent light easterly flow between 700-500 hPa countering the daytime mountain-valley circulation.

The final study (under revision in *Weather and Forecasting*) assesses composite atmospheric sounding analysis to forecast Air Quality Index ozone classifications of Good, Moderate, and collectively categories exceeding the U.S. EPA 2015 standard. The analysis, using Phoenix 12Z rawinsonde data (2006-2017), identifies the existence of "pollutant dispersion windows" for ozone accumulation and dispersal in Phoenix.

Ultimately, monsoon hazards result from a complex and evolving vertical atmosphere. This dissertation demonstrates the viability using available in-situ vertical upper-air data to anticipate recurring atmospheric states contributing to specific hazards. These results will improve monsoon hazard prediction in an effort to protect public and infrastructure.

DEDICATION

I dedicate this work to my family whose unwavering love and support have and always will be a source of inspiration. To my mother Annemarie Malloy, father William Malloy Jr., and brother Daniel Malloy, for embracing my passion for the weather. You all have laid a strong and loving foundation for me to pursue my curiosity of nature. I am grateful to share my journey with you.

ACKNOWLEDGMENTS

I thank Dr. Randall Cerveny for being a mentor and role model to me in academia and life. His continued guidance and support throughout my college and professional careers have truly made me a better person. Thank you for sharing your insight with me.

I thank my committee Dr. Nancy Selover, Dr. Anthony Brazel, and Dr. Robert Balling Jr. for all the thoughtful discussions and assistance as I progressed through my program at Arizona State University. Our interactions have made my experience at ASU memorable and positive. I also thank Dr. Matthew Pace for being a colleague, motivator, and friend.

Finally, I thank those who have sacrificed while encouraging me to follow my dreams.

TABLE OF CONTENTS

CHAPTER Page

LIST OF TABLES

LIST OF FIGURES

CHAPTER 1

INTRODUCTION

Monsoon Hazards

The American Southwest experiences what has been termed a "precipitation singularity" (Adams and Comrie, 1997; Sheppard et al., 2002) that occurs during the region's warm season having a defined date range between June 15 and September 30 (Sampson and Pytlak, 2008). A singularity is a reoccurring climatological event that becomes evident around a particular calendar date. The Monsoon signal criterion, defined by Ramage (1971), requires a summer prevailing wind shift of at least 120 degrees occurring at the low and mid-levels of the atmosphere. Tang and Reiter (1984) confirmed a monsoon existence over the large area encompassed by the Mexican Plateau and the United States Colorado Plateau; hence the precipitation singularity over the American Southwest is often referred as the North American Monsoon (NAM).

A defining synoptic feature for NAM is an anticyclonic circulation in the mid-levels of the atmosphere being a key mechanism for drawing moisture into the region. Strength and position of the monsoon circulation is significant for dictating local and large-scale wind fields focusing moisture advection from the eastern Pacific Ocean and Gulf of California (Adams and Comrie, 1997; Douglas et al., 1993) and Gulf of Mexico (Ellis and Saffell, 2004). Moisture interacts with strong surface heating and complex terrain throughout the region to provide high spatial and temporal variability for thunderstorm activity.

The onset of the NAM represents an important seasonal transition for the inhabitants of the southwestern United States. Monsoonal conditions are catalysts for severe weather thereby posing a risk to the community, economy, and environment of the region. For instance, the general public, ground transportation infrastructure, aviation, tourism attractions, agricultural activities, and recreational event planning are all sensitive to hazardous weather ranging from deadly dust storms, frequent lighting, life threatening flash flooding, dangerous thunderstorm downdraft winds, and damaging hail (e.g., Brazel and Nickling, 1986; Balling and Brazel, 1987; Desilets et al., 2008; King and Balling, 1994; Maddox et al., 1995; Raman et al., 2014; Wallace et al., 1999). Severe weather during the monsoon season has been documented to develop locally with little to no warning (McCollum et al., 1995). Adding to identified weather hazards are those non-meteorological in nature, specifically heat related illness (e.g., Harlan et al., 2006) and air quality deterioration affecting public health, such as from inhalation of suspended particulate matter from dust storm activity (Goudie, 2014; Middleton, 2017) or excessive ozone concentration exposure (e.g., Ellis et al., 2000; Shi et al., 2012).

The complexity of a monsoon climate having a broad spectrum of hazards recurring over a diverse geographical landscape, physically and culturally, demands attention for scientific inquiry. Obviously, a dynamically changing atmosphere has inherent forecasting challenges when identifying and anticipating those ideal conditions supportive of hazard development, whether meteorological or non-meteorological. Due to threat to life and property apparent by discussed monsoon risks without a complete understanding in the present-day literature, the opportunity for research focusing on particular subsets of hazards over different regions is both valid and necessary.

Although targeted research efforts are essential for refining early warning and forecast capability of monsoon hazards, a significant obstacle in the southwestern U.S. is the limited in-situ vertical sampling of the atmosphere (i.e., limited rawinsonde information). With this consideration, the overarching aim for the body of work presented in this dissertation is to investigate linkages between the monsoon atmosphere and hazard development by taking advantage of available Arizona upper air measurement sampling data in conjunction with available datasets documenting the observance of specific monsoon hazards.

Ultimately, the results discussed by this dissertation help build upon the evolving monsoon literature. Explicitly, synoptic atmospheric alignments and vertical atmospheric parameters for temperature, moisture, and wind characteristics are investigated for two independent hazard types, each at different locations. The first hazard is severe hail occurrence over the relatively unexplored and large Arizona portion of the Colorado Plateau by using Flagstaff sounding data and the National Climatic Data Center's Storm Events Database to identify days documenting ground reports of severe hail. The second investigation, broken into two distinct parts, involves surface ozone exceedance potential over the major Phoenix metropolitan area by reviewing Phoenix sounding data and the United States Environmental Protection Agency's (U.S. EPA) Air Quality System database to determine days when the daily maximum eight-hour ozone average concentration (DMO8) exceeded the U.S. EPA's National Ambient Air Quality Standards (NAAQS) for unhealthy air.

Problem Statement

There remain numerous potential monsoon hazard exploration studies capable of narrowing present knowledge gaps to our holistic understanding of the NAM. If the study of upper-air data is essential to our interpretation of monsoonal characteristics then using it to analyze completely independent aspects of the monsoon would demonstrate its versatility as a forecasting tool. Consequently, I have focused on severe hail over the Colorado Plateau and ozone accumulation variability in the Phoenix metropolitan area. These represent two unequivocally distinct monsoon hazards, one meteorological and the other air quality. Logistically, both areas of interest host routine sounding launches (i.e., Flagstaff and Phoenix) to facilitate interrogation of atmospheric parameters. Moreover, there is a documented history for both these hazards impacting populations with continued regularity in respective study areas.

Concerning severe hail on the Colorado Plateau, comprehensive evaluations of severe weather hazards tied to Arizona rural zones found in northern portions of the state are lacking, likely due to a sparse observation network existing in this vast and often considered remote territory (Sheppard et al., 2002). However, according to the National Climatic Data Center (NCDC) Storm Events Database, the Colorado Plateau has recorded many of the different types of severe weather during the monsoon, including severe hail, which has resulted in significant monetary damages. Studies directed at investigating convective environments leading to thunderstorms reaching severe thresholds over the Colorado Plateau would aid in filling a NAM literature gap, while also serving to support operational forecasting responsibility and public warning efforts by the National Weather

Service Forecast Office Flagstaff. The approach of analyzing atmospheric profiles supportive of severe hail for the Colorado Plateau has not been done to date.

Specific to ozone research, there have been numerous Phoenix ozone studies related to the spatial and diurnal patterns of ozone (e.g., Ellis et al., 2000; Shaw et al., 2005) and even work determining the presence of a “weekend effect” in the urban core (e.g., Shutters and Balling, 2006). However, a systematic review of recurring monsoonal atmospheric profiles that help or hinder ozone concentration potential remains absent from the literature. Separating key meteorological variables unique to different ozone ranges and not just near-surface parameters, which have been the focus of ozone studies to date (e.g., Alghamdi et al., 2014; 2014; Ellis et al., 1999; Ellis et al., 2000; Rasmussen et al., 2012), will greatly aid our conceptual model for how the NAM is influencing summertime ozone concentrations.

The monsoon period also overlaps with a time of maximum ozone experienced in the heavily urbanized city of Phoenix (i.e., late spring through summer months). Ozone, a gaseous secondary pollutant (Atkinson-Palombo et al., 2006), has exceeded the U.S. EPA’s NAAQS regularly during this time of year. Recently, the U.S. EPA has lowered the DMO8 standard from 75 parts per billion (ppb) to 70 ppb (U.S. EPA, 2015). Consequently, there is higher likelihood for more frequent ozone exceedances in the Phoenix metropolitan area that has already been designated as an ozone nonattainment area by the U.S. EPA. Since the Phoenix Nonattainment Area (PNA) bolsters a significant population numbering near five million residents as of 2017 (U.S. Census Bureau, 2018) and the fact that elevated ozone can have detrimental health consequences for the general public (i.e., Atkinson-Palombo et al., 2006; Owens et al., 2017), it is vital that we seek an understanding of the environment promoting unhealthy ozone accumulation for predictive purposes.

Operationally, the Arizona Department of Environmental Quality (ADEQ) is the authority for issuing daily ozone air quality forecasts for the PNA (ADEQ, 2019). ADEQ issues High Pollution Advisories (HPAs) to the public when the DMO8 is forecasted to exceed the ozone NAAQS for any monitor within the PNA. HPA days trigger announcements encouraging the public to limit outdoor activities, carpool, telecommute, measures to curb individual pollutant contribution, and other health conscious actions to take. Research oriented to identifying the common atmospheric states supportive of unhealthy ozone would assist confidence, accuracy, and lead time when forecasting ozone air quality episodes.

Whether it is severe hail or unhealthful ozone, forecasting during the NAM has proven difficult due to atmospheric conditions of temperature, moisture, and wind patterns being in constant flux as a result of an unstable monsoon circulation. For instance, over the course of the summer months, cycles of dry and wetter periods, referred to as “break” and “bursts” (Carleton, 1986), can take place on the order of a few days (Heinselman and Schultz, 2006) yet may potentially last over two weeks in duration (Mullen et al., 1998). A driving force behind the inconsistency in active weather has been linked to the ever-shifting Arizona monsoon boundary (Adang and Gall, 1989) largely dictated by the monsoon circulation (Moore et al., 1989). In general, this dividing line typically separates from the surface up to the midlevels of the atmosphere an unstable warm and moist air mass on its eastern side from a stable, cool, and drier air mass originating from the Pacific west of the demarcation zone.

Consequently, the evolution of the monsoon circulation through the atmospheric column could not only influence the placement of the Arizona monsoon boundary affecting instability required for thunderstorm formation and severe hail, but control general dispersion patterns for ozone above and near the surface, as well. The placement of the monsoon vertical circulation is likely a critical consideration for research investigating meteorological and non-meteorological hazards. Furthermore, this aspect underscores that studies restricted to surface analyses are likely to be inadequate by not relating evolving atmospheric conditions aloft. In other words, applying available upper-air measurements is fundamental for monsoon research in the U.S. Southwest.

Hypotheses

Broadly expressed, I hypothesize that, as a variable monsoon circulation "wobbles" both in strength and position over the U.S. Southwest, there will exist recurring and distinct patterns in the vertical structure of the atmosphere relative to the Colorado Plateau and the Phoenix metropolitan area that favor severe hail development and elevated ground-level ozone concentrations.

Explicitly for severe hail, occurrences will demonstrate a vertical profile indicative of a monsoon circulation placement offset toward the east of the Colorado Plateau that draws low-level moisture into the region from the south and southeast around the periphery of the anticyclone. The offset location also prevents strong subsidence aloft inherent with the upper-atmospheric anticyclone center that typically suppresses thunderstorm development. Additionally, the eastward shift in the anticyclone would allow possible intrusion of cooler air aloft from Pacific troughing over the western U.S.

to aid in destabilizing the atmosphere for thunderstorms to reach severe limits. As a result, I hypothesize a profile revealing warm, moist low and mid-levels with southeasterly advection occurring beneath a drier, cooler upper atmosphere with southwesterly flow; a combination that represents an unstable convective vertical profile.

Concerning ozone concentrations in Phoenix, I first hypothesize that there will exist an array of sounding parameters above the surface that show statistically significant differences in association with unhealthy and healthy ozone days. Specifically, variables will include temperature, moisture, wind speed. Ultimately, vertical atmospheric traces suitable for enhanced ozone accumulation in the PNA would depict a monsoon circulation nearly centered overhead. Placement would create 1) a weak pressure gradient to lower wind speeds and pollutant dispersion throughout column and 2) limit thunderstorm activity and cloud cover to interfere with sunlight necessary for new ozone formation. Therefore, periods of high ozone would follow “burst” and “break” periods in rainfall.

Furthermore, concerning ozone dispersion, wind speed versus prevailing wind direction, especially in the planetary boundary layer, is reasoned to play a larger role. This conjecture is based on prior studies indicating a persistent mountain-valley circulation in the Phoenix area during the monsoon period (Ellis et al., 1999).

Following confirmation that significant sounding parameters exist to differentiate days when ozone will exceed the U.S. EPA standard, I next hypothesize that by using atmospheric composite sounding analysis, I can identify common vertical profiles that exist for varying ranges of observed ozone concentrations in Phoenix.

Fundamentally, I hypothesize that statistical significance for geopotential height, air temperature, dew point, dew point depression, wind speed, and wind direction parameters extending throughout the atmospheric column, as measured by soundings, will be found in association with severe hail and ozone accumulation environment identification. Therefore, sounding data will be viable tools to forecast these hazards by finding ideal atmospheric combinations highlighting risk potential.

Dissertation Framework

Since the intention of this research is determining the viability for using limited in-situ sounding data in the American Southwest as potential tools to forecast a variety of meteorological and non-meteorological monsoon hazards, the following chapters contain three exploratory studies with a regional emphasis having a representative sounding site location. The three research endeavors attempt to establish the applicability for anticipating 1) severe hail formation over northern Arizona and 2) unhealthy ozone in central Arizona by employing Flagstaff and Phoenix sounding data, respectively. The central Arizona ozone exploration is divided into two studies as it was necessary to first establish whether or not any statistically significant meteorological variables above the planetary boundary layer are present with regard to unhealthy ground-level ozone concentrations. This distinction was not necessary for the severe hail study as it is already well-known that knowledge of tropospheric conditions is essential to thunderstorm prediction (e.g., King and Kennedy, 2019; Evans et al., 2018; Rodriguez and Bech, 2018). For ozone, once the significance of upper-air parameters was confirmed for exceeding versus non-exceeding ozone days, a second research paper begins to address the interplay between vertical temperature, moisture, and wind measurements using the composite atmospheric sounding analysis technique applied to specific ozone range breakpoints based on expected health impact determined by the U.S. EPA.

Chapter 2 comprises a published research paper discussing the applicability using Flagstaff, Arizona, 12Z (0500 LST) rawinsonde data to investigate morning atmospheric conditions preceding severe hail formation in the Arizona Colorado Plateau region during the monsoon season as cited by the National Climatic Data Center's Storm Events Database. I explicitly find statistically significant sounding parameters and thresholds unique to observed severe hail days versus documented non-severe hail days. Environmental conditions are discussed in relation to atmospheric instability and wind characteristics. This is a solo authored study published in the *Journal of the Arizona-Nevada Academy of Science* in 2011 (Volume 43(1); 16-26).

Chapter 3 incorporates a published research paper with focus on determining morning and afternoon (0500 and 1700 LST) statistically significant Phoenix sounding data parameters that distinguish healthy versus unhealthy daily maximum ozone concentrations observed in the Phoenix Nonattainment Area (PNA). The latest 2015 ozone standard set by the U.S. Environmental Protection Agency (U.S. EPA) is used as the division between healthy and unhealthy ozone days for the study period. Additionally, I use 1) principal component analysis (PCA), 2) linear discriminant analysis (LDA), and 3) synoptic composite analysis to aid in identifying common monsoon weather patterns favoring or limiting ozone accumulation potential in the PNA. This is a solo authored paper published in the journal *Atmospheric Environment* in 2018 (Volume 191; 64-69).

Chapter 4 constitutes a submitted research paper expounding upon original research discussed in Chapter 3. Specifically, composite sounding analysis for 12Z (0500 LST) Phoenix rawinsonde data is employed to find recurring atmospheric profiles differentiating three different tiers of daily maximum ozone concentration ranges observed in the PNA. Each of the three tiers in the study have broad implications for public health and correspond to the U.S. EPA's Air Quality Index (AQI) categories of Good, Moderate, and those categories that would exceed the daily U.S. EPA health standard. Representative composite soundings found for each tier are discussed in themes relative to moisture, temperature, and wind characteristics. The authors for this research are Jonny W. Malloy and Randall S. Cerveny. The article is under revision with the journal *Weather and Forecasting*.

Chapter 5 concludes the dissertation. First, I briefly review my research intent and hypotheses. Second, I summarize findings for the three research studies and discuss the significance of the results. I then examine whether my hypotheses are supported. Finally, the overall significance of my research is stated.

Beginning with a review on severe hail in the Colorado Plateau, the following three chapters present three separate studies providing evidence that ideal local atmospheric states using available sounding data in context with broader synoptic weather patterns can provide support when forecasting adverse meteorological conditions and air quality degradation impacting Arizona during the North American Monsoon.

CHAPTER 2

MONSOON SOUNDING PARAMETERS ATTRIBUTED TO SEVERE HAIL FORMATION ON THE COLORADO PLATEAU

This chapter investigates vertical atmospheric profiles supportive of monsoon related severe hail occurrences on the Arizona portion of the Colorado Plateau between 1996 and 2009. A version of this chapter titled: Using atmospheric profiles to forecast severe hail events in northern Arizona during the North American Monsoon season was published in the published in the *Journal of the Arizona-Nevada Academy of Science* in 2011 (Volume 43(1); 16-26). This was a solo authored study.

Abstract

Although it is a rare phenomenon, hail on the Colorado Plateau can be a significant hazard. This study identifies threshold values of specific atmospheric variables associated with observed severe hail occurrences for northern Arizona during the North American Monsoon seasons associated with the 1996-2009 timeframe. The threshold constraints on hail are found by constructing long-term means of the overall, non-severe hail, and severe hail atmospheric environments over northern Arizona, based on Flagstaff, Arizona, 12Z rawinsonde data. Results indicate that days experiencing severe hail possess a significantly different morning atmospheric profile. Key variations between days with severe hail versus days without severe hail are elevated sub-300 hPa moisture, a warmer atmosphere, lighter above surface wind speeds, more southerly to southeasterly oriented winds throughout the atmospheric column (except at the 700 hPa

pressure level), and noticeably higher geopotential heights at all mandatory pressure levels. Large-scale synoptic patterns associated with the North American Monsoon are the driving force behind whether a severe hail or non-severe hail environment exists over northern Arizona.

Introduction

The North American Monsoon (NAM) has been extensively reported upon (Adams and Comrie, 1997; Sheppard et al., 2002). The NAM specifically impacts the southwestern United States and northwestern Mexico on an annual basis during the summer months. This period is marked by an upswing in convective activity and associated precipitation that may affect diverse biomes ranging from elevated ponderosa pine forests down to the lower deserts (Diem and Brown, 2009; Michaud et al., 1995; Rowe et al., 2008). Generally, there is a northward propagation of observed monsoonal conditions beginning in northwestern Mexico in June followed by an expansion to an area roughly bounded by 41°N latitude and 105°W longitude (Adams and Comrie, 1997; Douglas et al., 1993). The shift from dry pre-summer conditions to relatively wet monsoon conditions is significant for the region as it has the potential to deliver over half of the annual precipitation to the area with a higher percentage being achieved closer to Mexico (Mitchell et al., 2002).

Severe weather is prevalent during the NAM season. Hazards associated with the season's frequent convective activity include damaging winds, dust storms, large hail, lightning, and flash flooding (e.g., Brazel and Nickling, 1986; Maddox et al., 1995; McCollum et al., 1995; Watson et al., 1994; Wallace et al., 1999). Evaluations by the

National Severe Storms Forecast Center (NSSFC), from the use of a forecast verification technique called the Critical Success Index (CSI), show that severe weather can often be missed by National Weather Service forecasters in this region (Maddox et al., 1995) due to some of these severe episodes occurring with little to no warning (McCollum et al., 1995). In regard to public safety, research concerning the identification of precursors leading to severe weather formation is necessary to provide ample warning time.

For Arizona, previous research concerning severe weather during the NAM has been primarily focused on the densely populated lower desert regions, particularly the Phoenix, Arizona, metropolitan area (McCollum et al., 1995; Wallace et al., 1999). This is reasonable given the magnitude of population that could be affected by such a study area (Heinselman and Schultz, 2006). Detailed evaluations of severe convection for other regions of Arizona are largely absent from the literature possibly due lack of documented severe cases (Maddox et al., 1995). However, since the mid-1990s, there has been an increase in severe weather reports, even in remote locations outside the large Phoenix metropolitan area. This is particularly true for northern Arizona. Consequently, this study is designed to access the variables that best indicate severe weather associated with the NAM by focusing on the atmospheric parameters that have preceded severe hail events in northern Arizona. It is anticipated that the results of this research will primarily aid operational forecasts generated for the NAM season by the National Weather Service Office Flagstaff located in central northern Arizona.

Data and Methods

Northern Arizona occupies 65,978.12 square miles and currently has a population around 650,000 people (U.S. Census Bureau, 2010). My study area includes the counties of Apache, Coconino, northern Gila, Mohave, Navajo, and Yavapai, containing the major cities of Flagstaff, Payson, Prescott, Show Low, and Winslow (Fig. 2.1). This region is part of the county warning region of the National Weather Service (NWS) Office in Flagstaff. The NWS Office Flagstaff is explicitly responsible for the following counties in Arizona: Apache, Coconino, northern Gila (Zone 018), Navajo, and Yavapai. The study area for northern Arizona was expanded to also include Mohave County (northwest corner of state and under the Las Vegas NWS Office jurisdiction) as it completes the northern Arizona territory, while maintaining distance symmetry with the Flagstaff rawinsonde site.

Since 2008, the National Weather Service in Arizona has established a fixed-length NAM season that extends from June 15 to September 30 (Sampson and Pytlak, 2008). For this study I extracted data for the period from 1996-2009 for a total time period of 1,512 days for the study area. Data consisted of: 1) 12Z rawinsonde data for Flagstaff prepared by the National Climatic Data Center's (NCDC) Integrated Global Radiosonde Archive (Gaffen, 1996) and 2) severe hail reports provided by the NCDC's Storm Event database (NCDC Storm Events, 2010). Rawinsonde data were only available for 1,450 days, which represents 95.9% of the possible study period. As documented by the NCDC's Storm Event database northern Arizona had 265 NAM related severe hail (using a criterion of hail that is at least 0.75 inches in diameter) events, or 149 individual days occurring between 1996 and 2009.

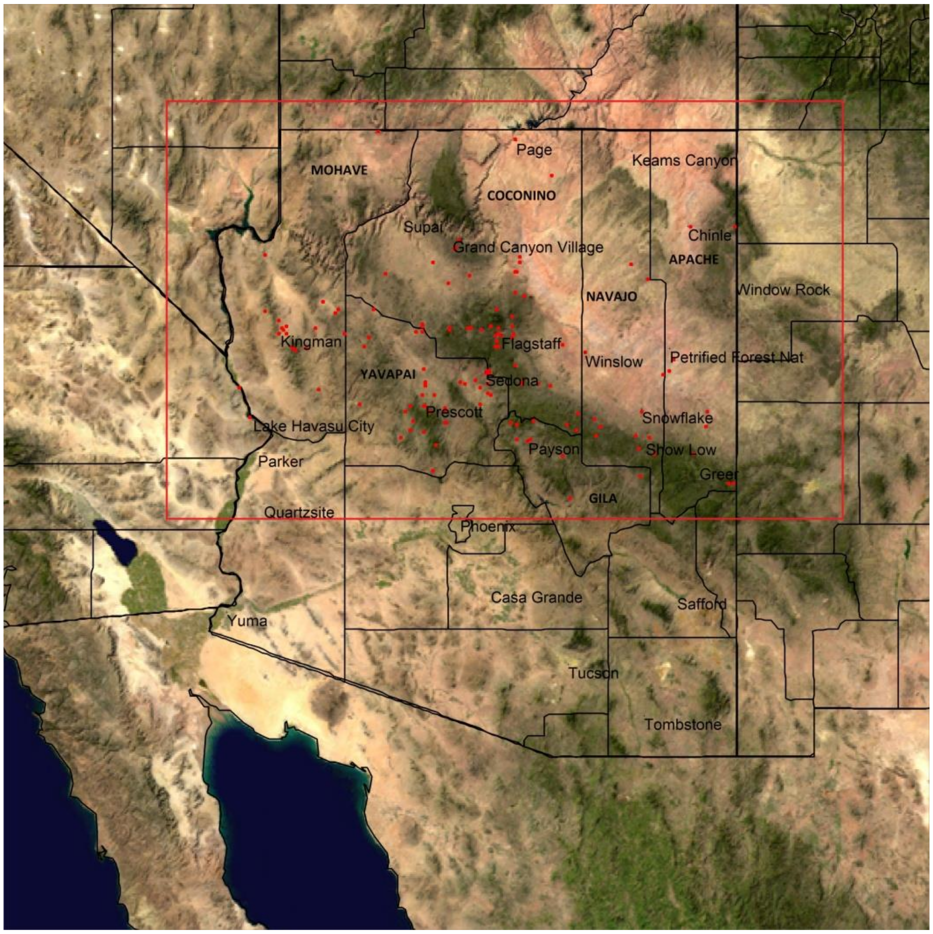

Fig. 2.1. Spatial distribution of northern Arizona NAM related severe hail reports from 1996-2009 (red dots). Northern Arizona study area (large red boxed region) includes Apache, Coconino, northern Gila, Mohave, Navajo, and Yavapai counties in Arizona. Flagstaff (top center) marks location of rawinsonde site.

Since the goal of this research is to establish the threshold levels of variables associated with potential severe hail episodes based on the 12Z sounding, any severe hail reported before 12Z on a particular day was discounted. This had only minor implications as such reports only represented 1.5% of all reports (Table 2.1). The temporal distribution of reported severe hail fits well with the established diurnal nature of convection (Adams and Comrie, 1997; Balling and Brazel, 1987; Bhushan and Barros, 2007; Rowe et al., 2008). Ultimately, report reductions in combination of missing rawinsonde data made the final dataset to consist of 1,450 days with 139 days observing severe hail.

Table 2.1
Diurnal variations of NAM related severe hail reports for the northern Arizona study area identified in the text (1996-2009).

Number of Reports (total *n*-size 265)	Time of Occurrence	Percent of Reports
4	<12Z	1.5
203	12-00Z	76.6
58	>00Z	21.9

To aid in distinguishing between days with potential severe hail events versus those with no severe hail it was necessary to construct three mean 12Z soundings based on 42 atmospheric parameters consisting of the averaged values for geopotential height, temperature, dewpoint, dewpoint depression, wind direction, and wind speed found at the surface and the mandatory pressure levels up to 200 hPa from all available soundings. From the resultant 42 parameters three classes of soundings were created: 1) the mean 12Z NAM (includes all 1,450 soundings regardless of the observance of hail or no hail), 2) the mean 12Z non-severe hail days (1,311 soundings), and 3) the mean 12Z severe hail days (139 soundings). By ingesting the averaged rawinsonde data in the RAwinsond OBservation Program (RAOB), developed by Environmental Research Services, LLC., these soundings could then be visualized (Fig. 2.2).

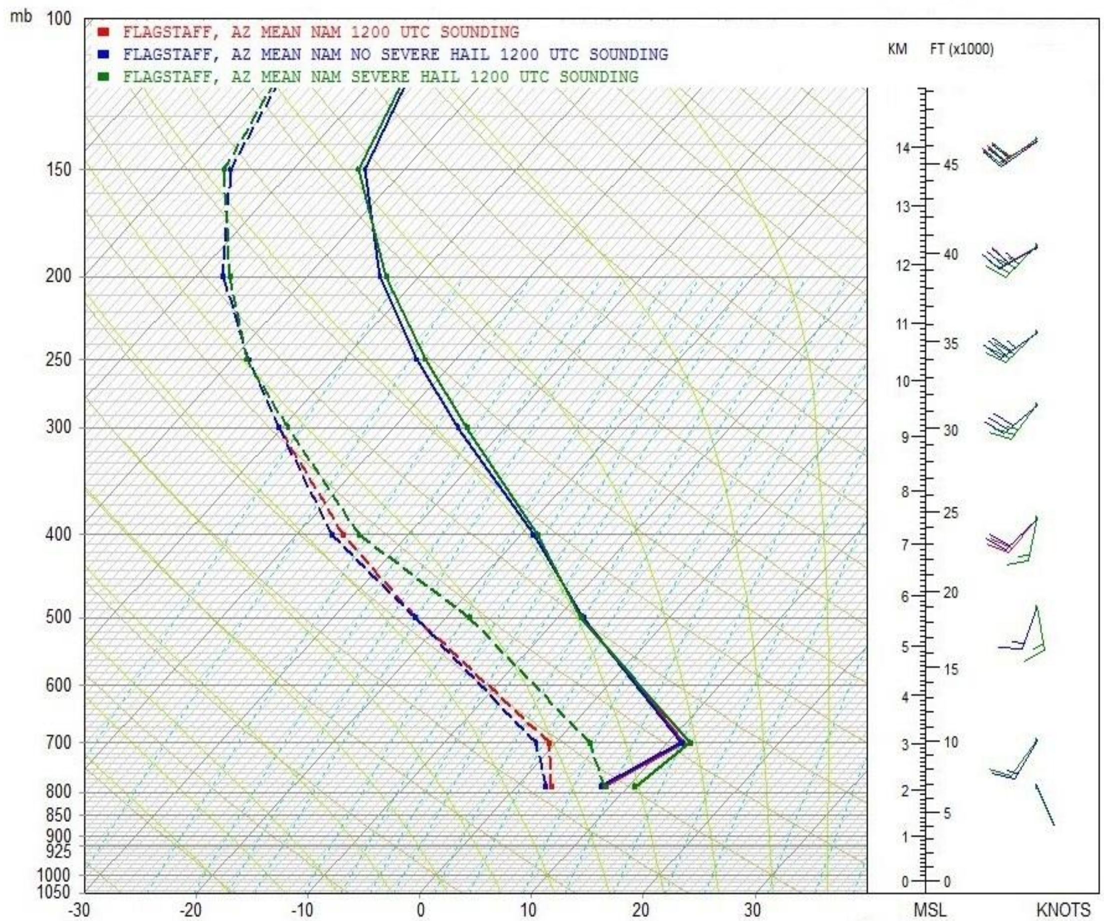

Fig. 2.2. Skew T-log p thermodynamic composite plot of the 14-year mean 12Z Flagstaff soundings for NAM all days (red sounding), NAM non-severe hail days (blue sounding), and NAM severe hail days (green sounding).

Results and Discussion

The "unequal variance t-test," or also known as the Smith-Welch-Satterwaite test (Ruxton, 2006), was used in this study to determine whether or not statistically significant differences existed between values for 42 atmospheric variables occurring on non-severe hail days versus severe hail days. The Smith-Welch-Satterwaite test is a parametric test that was designed to allow statistical comparisons for groups of data with uneven n-sizes and very different variances (Ruxton, 2006). The test statistic, *t*, is calculated from

$$t' = \frac{\mu_1 - \mu_2}{\sqrt{\frac{s_1^2}{n_1} + \frac{s_2^2}{n_2}}} \quad (1)$$

and the degrees of freedom, *v*, from

$$v = \frac{\left(\frac{1}{n_1} + \frac{u}{n_2}\right)^2}{\frac{1}{n_1^2(n_1-1)} + \frac{u^2}{n_2^2(n_2-1)}} \quad (2)$$

where *n* is sample size, *u* is mean, *s* is variance, and *u* is

$$u = \frac{s_2^2}{s_1^2} \quad (3)$$

Although the data used in this study showed some deviations from normality determined from the Probability Plot Correlation Coefficient test for normality (Filliben, 1975; Vogel, 1986), use of the parametric Smith-Welch-Satterwaite test is still valid given the large sample sizes (n-sizes much greater than 30) for this study (Burt and Barber, 1996; Ruxton, 2006) and previous research demonstrating that the Smith-Welch-Satterwaite test should be implemented in place of the nonparametric Mann-Whitney U test (Ruxton, 2006).

Analysis has revealed that values for 30 of the study's 42 atmospheric variables found on morning soundings, preceding severe hail in northern Arizona during the NAM, are statistically different at the 95% confidence level (α value of 0.05) than values associated with non-severe hail days (Table 2.2). Additionally, 22 of 42 variables were statistically different at the 99% confidence level (α value of 0.01).

Table 2.2

Smith-Welch-Satterwaite test statistical results found when comparing values of selected 12Z Flagstaff sounding atmospheric variables associated with non-severe hail days versus severe hail days observed over northern Arizona during the North American Monsoon seasons spanning 1996-2009. Values given include mean, *n*-size, variance, calculated degrees of freedom (v), Smith-Welch-Satterwaite test statistic (t), and *p*-value indicating the probability that values for a given variable between non-severe hail days and severe hail days are different. Units for temperature (T), dewpoint (Td), and dewpoint depression (Tdd) are in °C, knots for wind speed (WS), degrees for wind direction (WD), and meters for geopotential height (GPH).

Variable	Mean (Non-SH)	Mean (SH)	*n* (Non-SH)	*n* (SH)	Var (Non-SH)	Var (SH)	*v*	*t*	*p* (different)
Surface T	7.70	10.6	1301	139	17.3	7.54	212	11.2	>0.999
Surface Td	2.57	7.93	1301	139	42.6	8.70	311	17.3	>0.999
Surface Tdd	5.13	2.70	1301	139	19.7	5.84	252	10.1	>0.999
700 hPa Td	-1.78	3.33	1307	139	54.2	12.0	295	14.3	>0.999
700 hPa Tdd	13.1	8.59	1307	139	65.8	23.2	231	9.67	>0.999
500 hPa Td	-23.4	-17.6	1303	138	153	117	177	5.85	>0.999
500 hPa Tdd	15.6	9.78	1303	138	161	122	177	5.84	>0.999
250 hPa T	-43.5	-42.7	1290	135	6.52	2.94	202	5.32	>0.999
200 hPa GPH	12372	12402	1284	135	7016	5218	174	4.51	>0.999
500 hPa WD	202	167	1288	136	6079	7836	157	4.33	>0.999
400 hPa WD	223	191	1284	137	5825	7820	158	3.99	>0.999
300 hPa T	-34.3	-33.6	1295	138	6.62	4.58	182	3.79	>0.999
250 hPa GPH	10905	10930	1289	135	5841	5117	167	3.76	>0.999
700 hPa WS	13.0	10.9	1292	136	69.3	39.6	188	3.51	0.999
200 hPa T	-53.5	-52.9	1284	135	5.10	3.54	177	3.44	0.999
300 hPa GPH	9655	9674	1294	138	4489	4118	170	3.35	0.999
700 hPa GPH	3170	3179	1311	139	1044	861	175	3.27	0.999
500 hPa GPH	5880	5893	1307	138	2081	1866	170	3.23	0.999
400 hPa GPH	7579	7593	1299	139	2773	2554	171	3.21	0.998
400 hPa WS	20.4	17.2	1284	137	173.9	119	181	3.20	0.998
300 hPa WS	28.3	24.7	1281	136	265	203	174	2.79	0.994
700 hPa T	11.3	11.9	1309	139	9.02	6.26	183	2.61	0.990

400 hPa T	-18.9	-18.5	1298	139	4.71	3.67	178	2.54	0.988
300 hPa WD	231	213	1281	136	4521	6603	155	2.42	0.983
400 hPa Td	-37.0	-34.6	1297	139	119	131	166	2.40	0.983
200 hPa WD	241	224	1250	132	3156	6454	144	2.32	0.979
500 hPa WS	16.8	14.9	1288	136	125	77.0	184	2.29	0.977
250 hPa WS	33.7	30.2	1267	133	319	293	163	2.22	0.972
200 hPa WS	36.7	33.2	1250	132	328	343	158	2.04	0.957
400 hPa Tdd	18.1	16.1	1297	139	115	126	166	2.01	0.954

Therefore, severe hail thresholds were established as the mean value found on the 139 severe hail soundings for the 30 statistically significant atmospheric variables. This made it possible to then analyze each sounding, whether it was associated with severe hail or non-severe hail, on an individual basis to discover how many, if any, of the 30 variables and type were present at severe levels. There are two categories compared: a) known severe hail days having variable(s) at severe criteria (Table 2.3) and b) non-severe hail days with variable(s) meeting severe thresholds (Table 2.4).

Table 2.3
Breakdown of statistically significant variables reaching severe hail thresholds on severe hail soundings. Values given are *n*-size, percentage of severe hail days, minimum and maximum value found from all severe hail soundings, and the severe hail threshold value for each variable. Units for temperature (T), dewpoint (Td), and dewpoint depression (Tdd) are in °C, knots for wind speed (WS), degrees for wind direction (WD), and meters for geopotential height (GPH).

Sig. Variable (α ≥ 0.05)	Days Meeting SH Threshold on Non-SH Soundings	*n* (Non-SH)	% of Non-SH Days	Min Sounding Value	Max Sounding Value	SH Threshold
500 hPa Tdd	98	138	71.0	0	48	≤9.78
500 hPa Td	94	138	68.1	-57.7	-6.7	≥17.7
250 hPa GPH	87	135	64.4	10584	11040	≥10930
Surface Tdd	87	139	62.6	0	15	≤2.71
300 hPa GPH	86	138	62.3	9357	9770	≥9675
400 hPa GPH	86	139	61.9	7337	7680	≥7594
500 hPa GPH	83	138	60.1	5682	5970	≥5893
250 hPa T	81	135	60.0	-47.9	-38.7	≥-42.7
200 hPa GPH	81	135	60.0	12063	12520	≥12402
700 hPa GPH	83	139	59.7	3035	3233	≥3179
250 hPa WS	79	133	59.4	1.9	72.8	≤30.3

400 hPa WS	80	137	58.4	0.9	61.9	≤17.3
700 hPa WS	77	136	56.6	0	32.1	≤10.9
300 hPa WS	75	136	55.1	0.9	62.9	≤24.7
700 hPa T	76	139	54.7	4.5	18.4	≤11.9
400 hPa T	76	139	54.7	-24.8	-14.6	≥-18.5
400 hPa Tdd	76	139	54.7	0.4	45	≤16.1
400 hPa Td	76	139	54.7	-62.3	-17.7	≥-34.6
200 hPa WS	72	132	54.5	5.8	82.9	≤33.3
Surface T	75	139	54.0	3.3	18	≥10.6
700 hPa Tdd	75	139	54.0	0.2	27	≤8.60
700 hPa Td	73	139	52.5	-12.2	10.7	≥3.33
300 hPa T	72	138	52.2	-40.7	28.5	≥-33.6
500 hPa WS	69	136	50.7	0.9	49.9	≤14.9
Surface Td	70	139	50.4	0.5	14.5	≥7.94
400 hPa WD	61	137	44.5	15	358	≤191
200 hPa T	59	135	43.7	-57.9	-46.5	≥52.9
500 hPa WD	59	136	43.4	0	350	≤167
200 hPa WD	48	132	36.4	0	355	≤224
300 hPa WD	48	136	35.3	0	355	≤213

Table 2.4

Breakdown of statistically significant variables reaching severe hail thresholds on non-severe hail soundings. Values given are *n*-size, percentage of non-severe hail days, minimum and maximum value found from all non-severe hail soundings, and the severe hail threshold value for each variable. Units for temperature (T), dewpoint (Td), and dewpoint depression (Tdd) are in °C, knots for wind speed (WS), degrees for wind direction (WD), and meters for geopotential height (GPH).

Sig. Variable (α ≥ 0.05)	Days Meeting SH Threshold on Non-SH Soundings	*n* (Non-SH)	% of Non-SH Days	Min Sounding Value	Max Sounding Value	SH Threshold
Surface Td	306	1301	23.5	-21	14.9	≥7.93
400 hPa WD	323	1284	25.2	0	356	≤191
700 hPa Td	334	1307	25.6	-12.2	10.7	≥3.33
200 hPa WD	336	1250	26.9	0	355	≤224
500 hPa WD	349	1288	27.1	0	358	≤167
300 hPa WD	359	1281	28.0	0	357	≤213
Surface T	369	1301	28.4	-3.7	21	≥10.6
700 hPa Tdd	424	1307	32.4	0.2	27	≤8.59
200 hPa T	493	1284	38.4	-61.1	-44.5	≥-52.9
400 hPa Td	530	1297	40.9	-65.1	-15.6	≥-34.6
200 hPa GPH	527	1284	41.0	12001	12550	≥12402
Surface Tdd	535	1301	41.1	0	24	≤2.70
500 hPa Td	539	1303	41.4	-57.9	-5.6	≥-17.6

500 hPa GPH	546	1307	41.8	5680	5976	≥5893
500 hPa Tdd	558	1303	42.8	0	49	≤9.78
300 hPa T	557	1295	43.0	-43.3	-22.5	≥-33.6
700 hPa T	572	1309	43.7	4.5	18.4	≥11.9
400 hPa GPH	574	1299	44.2	7330	7690	≥7593
300 hPa GPH	573	1294	44.3	9330	9791	≥9674
250 hPa T	573	1290	44.4	-53.2	-36.9	≥-42.7
250 hPa GPH	575	1289	44.6	10550	11054	≥10930
700 hPa GPH	586	1311	44.7	3035	3233	≥3179
400 hPa Tdd	585	1297	45.1	0.2	45	≤16.1
400 hPa T	590	1298	45.5	-27.3	-13.1	≥-18.5
300 hPa WS	595	1281	46.4	0.9	102.9	≤24.7
250 hPa WS	599	1267	47.3	0	105.8	≤30.2
200 hPa WS	592	1250	47.4	0	116.9	≤33.2
400 hPa WS	611	1284	47.6	0.9	159.8	≤17.2
700 hPa WS	621	1292	48.1	0	32	≤10.9
500 hPa WS	626	1288	48.6	0.9	104.9	≤14.9

Interestingly, zero of the 139 documented severe hail cases had all 30 severe parameters present, though every case had at least two variables meeting severe criterion and nearly 75% of these cases had anywhere from 11 to 29 present (see Table 2.3). The range for any one variable being severe on a severe hail day was 48-98 days out of 139 or 35.4% (Table 2.5). When focusing on non-severe hail soundings, it was found that a significant portion of these 1311 soundings (98.2%) exhibited severe criteria for at least one variable; however, only 32.3% of soundings demonstrated greater than 15 severe parameters (Table 2.5). The likelihood for a non-severe hail sounding to have a variable in the severe category was between 306-626 days out of 1,311 days or 23.5-48.6%.

Table 2.5
Occurrences of determined statistically significant variables reaching severe hail criteria on both severe hail days (left) and non-severe hail days (right).

# of Sig. Variables	SH Days Meeting ≥SH Criteria	% of SH Days	# of Sig. Variables	Non-SH Days Meeting ≥SH Criteria	% of Non-SH Days
0	0	0.0	0	23	1.8
1-5	12	8.6	1-5	318	24.3
6-10	23	16.5	6-10	299	22.8
11-15	26	18.7	11-15	248	18.9
16-20	34	24.5	16-20	221	16.9
21-25	29	20.9	21-25	157	12.0
26-29	15	10.8	26-29	45	3.4
30	0	0.0	30	0	0.0

The marked variability that exists for both comparisons makes it difficult to declare a single severe parameter as being more vital to severe hail formation than another. An attempt at a ranking system is still applied by taking the ratio between percentages that a severe parameter was present on severe hail soundings versus non-severe hail soundings (Table 2.6). Higher ratios (>1.0) points to severe parameters being more linked with severe hail events than non-severe hail since such a ratio means a severe parameter is more prevalent, proportion wise, for severe hail soundings compared to non-severe hail soundings. Relatively lower ratios (≤1.0) would highlight instances where severe parameters have a) low occurrences on both sets of soundings, b) high occurrences for both severe hail and non-severe hail days, or c) is more dominant for a non-severe sounding. The purpose of the ranking system is to help isolate specific severe parameters associated with only severe hail days (higher ratios), which would identify that variable as being a greater contributor to severe hail formation. Since not one severe parameter occurred for every instance that a severe hail event transpired, it is likely that severe hail formation would rather rely on the interplay of multiple severe parameters, but it is apparent from Table 6 that occurrences of severe hail are weighted most heavily upon increased 500 hPa and surface moisture as well as higher geopotential heights between 700 hPa and 200 hPa.

Table 2.6

Ranking results after taking the ratio between percentages that a severe parameter was present on severe hail soundings versus non-severe hail soundings. Higher ratios (>1.0) points to severe parameters being more linked with severe hail events than non-severe hail since such a ratio means a severe parameter is more prevalent, proportion wise, for severe hail soundings compared to non-severe hail soundings. Relatively lower ratios (≤1.0) would highlight instances where severe parameters have a) low occurrences on both sets of soundings, b) high occurrences for both severe hail and non-severe hail days, or c) is more dominant for a non-severe sounding.

Rank	Sig. Variable ($\alpha \geq 0.05$)	% of SH Days Meeting SH Threshold	% of Non-SH Days Meeting SH Threshold	Ratio	SH Threshold
1	Surface Td	50.4	23.5	2.14	≥7.93
2	700 hPa Td	52.5	25.6	2.06	≥3.33
3	Surface T	54.0	28.4	1.90	≥10.6
4	400 hPa WD	44.5	25.2	1.77	≤191.8
T-5	700 hPa Tdd	54.0	32.4	1.66	≤8.59
T-5	500 hPa Tdd	71.0	42.8	1.66	≤9.78
7	500 hPa Td	68.1	41.4	1.65	≥-17.6
8	500 hPa WD	43.4	27.1	1.60	≤167.9
9	Surface Tdd	62.6	41.1	1.52	≤2.70
10	200 hPa GPH	60.0	41.0	1.46	≥12402
T-11	250 hPa GPH	64.4	44.6	1.44	≥10930
T-11	500 hPa GPH	60.1	41.8	1.44	≥5893
13	300 hPa GPH	62.3	44.3	1.41	≥9674
14	400 hPa GPH	61.9	44.2	1.40	≥7593
T-15	200 hPa WD	36.4	26.9	1.35	≤224
T-15	250 hPa T	60.0	44.4	1.35	≥-42.7
T-17	400 hPa Td	54.7	40.9	1.34	≥-34.6
T-17	700 hPa GPH	59.7	44.7	1.34	≥3179
T-19	300 hPa WD	35.3	28.0	1.26	≤213
T-19	250 hPa WS	59.4	47.3	1.26	≤30.2
21	700 hPa T	54.7	43.7	1.25	≥11.9
22	400 hPa WS	58.4	47.6	1.23	≤17.2
T-23	300 hPa T	52.2	43.0	1.21	≥-33.6
T-23	400 hPa Tdd	54.7	45.1	1.21	≤16.1
25	400 hPa T	54.7	45.5	1.20	≥-18.5
26	300 hPa WS	55.1	46.4	1.19	≤24.7
27	700 hPa WS	56.6	48.1	1.18	≤10.9

28	200 hPa WS	54.5	47.4	1.15	≤33.2
29	200 hPa T	43.7	38.4	1.14	≥-52.9
30	500 hPa WS	50.7	48.6	1.04	≤14.9

It should be noted that since a vast majority of severe hail reports are clustered around cities and that northern Arizona occupies a large remote territory (see Fig. 1) it is certain that a number of severe hail events have gone unreported to the NCDC by taking place in blind spots that exist throughout the weather spotter network in the region. This could partially explain the unexpected high incidence of severe parameters noted by some “non-severe hail” soundings, but given that certain variables at severe thresholds are clearly more common than others when analyzing non-severe hail soundings, it could be reasoned that atmospheric conditions favorable for severe hail formation do not occur abruptly but rather build over a period of time until climaxing as a severe hail event. If so, then Table 6 could illustrate the progression, when viewed from bottom to top, leading up to severe hail episodes; where atmospheric winds decrease as geopotential heights and temperatures build followed by moistening of the atmosphere from the top down that is then accompanied by a south-southeasterly wind shift culminating in elevated surface moisture. Indeed, there are two main variations between severe and non-severe hail profiles that are grouped in the following categories: a) instability (temperature and moisture) and b) wind velocity (direction and speed of air flow).

Instability

The environment conducive for severe hail is found to be a relatively warmer and wetter atmosphere, particularly between the surface and the 500 hPa pressure level. Between these levels, and at the surface, temperature and dewpoint readings have a tendency to show increased values with corresponding lower dewpoint depressions when compared to non-severe hail profiles. This is linked to the significance of the boundary layer instability contributing to severe convective events. Convection developing during non-severe hail conditions is likely to be inhibited by a cooler and drier environment. Formation of convection in such conditions struggles to overcome dry air entrainment in its ascent, which suppresses further growth of any convection due to evaporative cooling lessening lapse rates and therefore stabilizing the atmosphere (e.g., Kirshbaum and Durran, 2004; Vasquez, 2010; Zehnder et al., 2006). The resultant negative buoyancy with no additional moisture or forcing mechanism will not allow convection to reach severe levels.

Wind Velocity

Another major difference found with unstable severe hail soundings is the direction and speed of air flow throughout the atmospheric column. Generally, at 200 hPa and below wind direction associated with severe hail profiles is found to be more south to southeasterly (except at 700 hPa pressure level) and register at slightly lighter velocities. The implications of a southeasterly wind versus a southwesterly wind affecting an individual thunderstorm are unclear, but would rather help explain the increased temperatures and moisture found in severe hail environments through advection.

The North American monsoon season is documented to be caused by a large-scale atmospheric shift of the mid- to upper-level subtropical high-pressure system (e.g., Adams and Comrie, 1997; Ellis et al., 2004; Johnson et al., 2007; Sheppard et al., 2002,). Research has shown that the farther north the midlevel subtropical high is positioned the greater the northward expansion of convective activity becomes, while a downtrend in convective activity north of Mexico is linked with a more southern position (Ellis et al., 2004). In response of the northward intrusion of the subtropical high a persistent trough forms to its west. This setup serves to draw midlevel and upper level moisture from the eastern Pacific, Gulf of California, and Gulf of Mexico (Mitchell et al., 2002; Higgins et al., 2004; Higgins and Shi, 2005; Sheppard et al., 2002,). This synoptic pattern would invoke south to southeasterly flow that would advect elevated temperatures and moisture (greater instability) with higher geopotential heights for all pressure levels to northern Arizona. Movement of the axis to the south allows intrusive dry and cool upper level air to approach from the west (Adams and Comrie, 1997). This explains the relatively cooler and drier conditions and southwesterly flow experienced during non-severe hail days along with lower geopotential heights at all pressure levels.

These large-scale patterns are not permanent and considerable research has addressed how variations of their displacement can alter precipitation throughout the region. During the course of the NAM, cycles of wet days and dry days, also known as “breaks” and “bursts,” respectively, are common (Carleton, 1986). These enhanced versus lull periods in storm activity could potentially last several days at a time (e.g., Adams and Comrie 1997, Carleton, 1986; Heinselman and Schultz, 2006; Mullen et al., 1998; Sheppard et al., 2002; Watson et al., 1994). Locations transitioning from a wetter to a drier atmosphere (or vice versa) can witness precipitable water rise and falls on the order of a half an inch over a very short time (Moore et al., 1989; Mullen et al., 1998). This notion holds true for this study as elevated moisture in terms of statistically higher dewpoints and lower dewpoint depressions are indicated by severe hail soundings. The axis of the midlevel subtropical high was found to be the main determining factor for whether a wet or dry regime exists (Heinselman and Schultz, 2006) and would also appear to be a main control when forecasting severe hail during the NAM (Fig. 2.3).

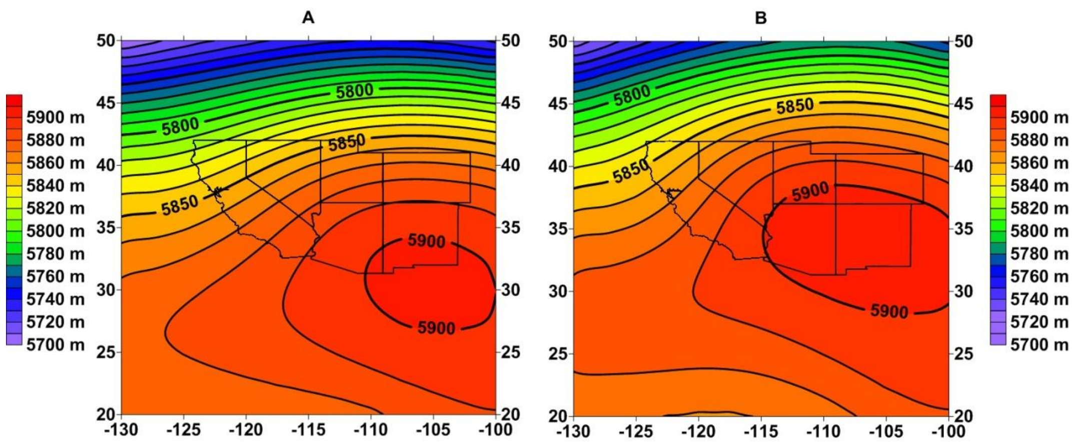

Fig. 2.3. Daily composites showing the 1996-2009 North American Monsoon 500 hPa synoptic pattern over the Southwest United States when northern Arizona experiences non-severe hail days (A) versus when severe hail events have been documented in northern Arizona (B). Note the northward expansion of the midlevel subtropical ridge during northern Arizona severe hail events. NCEP Reanalysis data were obtained to help construct daily composites (Kalnay, 1996).

The predominately southwesterly winds apparent at 700 hPa in both the severe hail and non-severe soundings is interesting. The southwest trajectory would likely advect a drier air mass at this pressure level. The mixing of upper level dry air with lower level moist air found in severe hail soundings has the potential to "overturn" due to density contrasts. This process has been documented as a severe weather ingredient over the Great Plains of the United States (Bunkers et al., 2010).

Conclusions

Results from this 14-year study indicate that morning air masses residing over northern Arizona during the NAM that are conducive for severe hail episodes reveal significant differences from air masses for those days with no severe hail as 30 of the 42 atmospheric variables used in this study were statistically different at the 95% confidence level or greater. Identifying the most critical variables specific for severe hail formation has proved difficult, but findings outlined in Tables 2.3 and 2.6 along with Figure 2.2 suggest that a favorable severe hail morning air mass over northern Arizona during the NAM would be distinguished from a non-severe hail morning air mass by having greater instability, related to enhanced low-mid tropospheric moisture, particularly at 500 hPa and the surface, along with a warmer atmosphere, coupled with southeasterly versus southwesterly advection that is likely to form in response to a northern shift of the subtropical high. As a result, severe hail events over northern Arizona would be tied to the transformation of large-scale synoptic patterns over the southwest United States.

Given the results, it does appear plausible to forecast daily severe hail events for northern Arizona based on 12Z Flagstaff rawinsonde data. As alluded to earlier current forecast skill during the NAM is limited. Conducting an evaluation to determine the atmospheric parameters corresponding to severe hail in northern Arizona should prove useful for 1) operational forecasters and 2) expanding our understanding of processes governing the behavior of the NAM and its associated severe weather.

CHAPTER 3

MONSOON VERTICAL ATMOSPHERIC PATTERNS AND UNHEALTHY OZONE LEVELS IN PHOENIX, ARIZONA

This chapter examines significant summertime sounding variables and synoptic patterns linked with unhealthy ozone accumulation in the U.S. Environmental Protection Agency designated Phoenix Nonattainment Area from 2006-2016. A version of this chapter titled: “Atmospheric patterns in relationship with observed ozone concentrations in the Phoenix, Arizona, metropolitan area during the North American Monsoon” was published in the published in the journal *Atmospheric Environment* in 2018 (Volume 191; 64-69). This was a solo authored study.

Abstract

Phoenix, Arizona is a designated ozone nonattainment area by the United States Environmental Protection Agency (EPA) and is susceptible to unhealthy ozone during the summer North American Monsoon. This study identifies common July and August synoptic environments linked with daily exceedances and non-exceedances of the EPA National Ambient Air Quality Standard (NAAQS). Results indicate a common weather pattern for exceeding the NAAQS consisting of 1) an amplified high-pressure ridge over the Four Corners region causing 500hPa heights to often exceed 5910 meters, 2) surface afternoon temperatures typically rising over 40°C, 3) lighter wind speeds in the planetary boundary layer (PBL) under four ms^{-1}, and 4) a distinct and persistent light easterly flow regime from 700-500 hPa. The last feature would counter local mountain-valley winds in

the upper PBL to promote ozone accumulation aloft and subsequent fumigation. Conversely, non-exceedance days are associated with 1) West Coast troughing and 500hPa geopotential heights between 5.9 to 21.4 meters lower, 2) afternoon PBL temperatures on average 0.8°C to 2.2°C cooler, 3) faster afternoon westerly flow at 925 and 850 hPa over four ms^{-1}, and 4) westerly flow in general at and above 925 hPa, aligning with the daytime mountain-valley circulation. Furthermore, a secondary non-exceedance pattern was identified. This less frequent pattern has moist southeast flow and is recognized for bringing widespread convective storm activity to central Arizona, including the PNA, based on prior research.

Introduction

Ground-level ozone is one of six criteria air pollutants deemed by the U.S. Environmental Protection Agency (EPA) to pose a risk to health and the environment. In an effort to regulate pollution levels the EPA has imposed pollutant specific National Ambient Air Quality Standards (NAAQS). Areas found to not meet pollutant standards are considered to be in nonattainment. The Phoenix-Mesa Mean Statistical Area (MSA) is designated as nonattainment for ozone (PNA hereafter) and occupies nearly 13,000 km^2 in south-central Arizona (Fig. 3.1). At the time of this study, the PNA had 20 regulatory monitors sited at a mix of urban, suburban, and rural locations. Terrain is complex in the PNA with elevation for monitoring sites varying between 258 and 1582 meters at the Buckeye ("BU") and Humboldt Mountain ("HM") sampling locations, respectively.

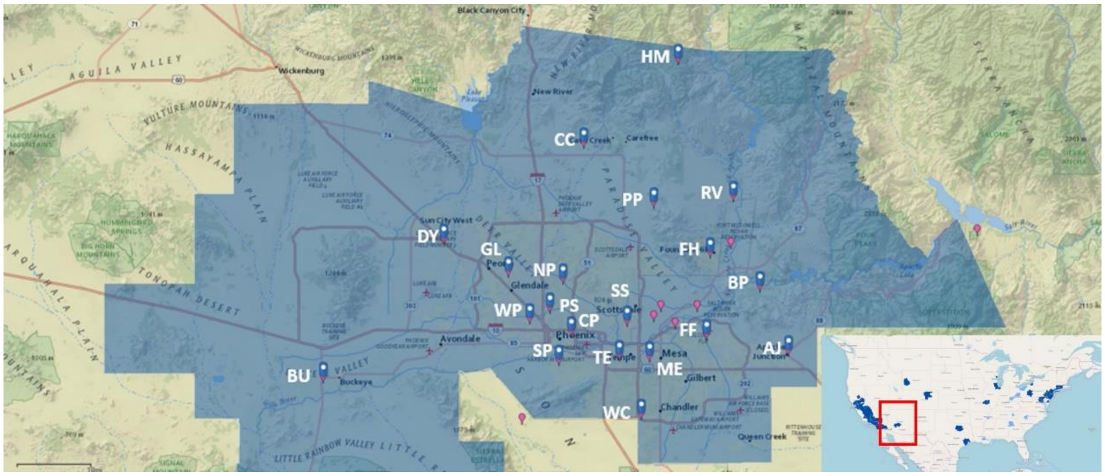

Fig. 3.1. Phoenix-Mesa MSA ozone nonattainment area (PNA) boundary (dark shade) with the 20 regulatory ozone monitors (listed in white letters) used in study denoted as balloon markers. Ozone monitors are overlaid with topography to highlight the complex terrain. Inset map of United States shows the PNA (within box) relative to other U.S. ozone nonattainment areas (dark polygons). Maps generated from EPA's website (U.S. EPA, 2017).

In 2015, the EPA lowered the ozone NAAQS to its latest adjustment, which is based on a daily maximum 8-hour average concentration (labeled as DMO8 in this study), from 75 parts per billion (ppb) to 70 ppb. Consequently, there is an expectation for more frequent daily ozone exceedances as the standard drops closer to mean concentrations typically observed in the PNA during the summer North American Monsoon (NAM) (Adams and Comrie, 1997) in the months of July and August (Fig. 3.2). Since the PNA hosts a significant population numbering over four million residents as of 2015 (U.S. Census Bureau, 2017) and ozone may have detrimental health consequences for the general public (e.g., Owens et al., 2017), it is vital for predictive purposes that we achieve a better understanding of atmospheric conditions supportive of unhealthful levels of surface ozone in this region.

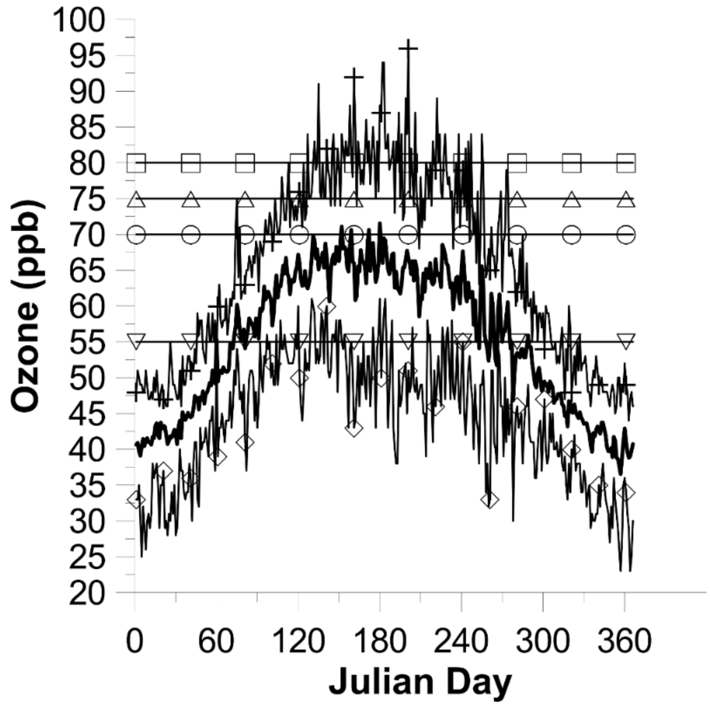

Fig. 3.2. Annual plot showing the 2006 to 2016 PNA mean (bold black line), maximum observed (plus sign), and minimum observed (diamond) DMO8 values. Additionally, the U.S. EPA 1997, 2008, and 2015 NAAQS ozone standards are indicated (square, triangle, and circle, respectively). Mean, maximum, minimum curves calculations are based only on the highest reporting daily DMO8 in the 20-monitor network for a given day. The NAM season covers the months of July and August and is the focus of this study.

Historically, meteorological forecasting in the southwest U.S. during the NAM phenomenon poses challenges due to a wide variation in atmospheric conditions throughout the season (Adams and Comrie, 1997; Sheppard et al., 2002). For example, marked intra-seasonal spatial differences for summertime precipitation have been observed to take place that is caused by the monsoon circulation intermittently deviating over relatively short periods thereby affecting moisture, temperature, winds, and overall atmospheric instability (e.g., Shi et al., 2012). Specifically, the monsoon consists of "breaks" and "bursts" (Carleton 1986) in regional rainfall. Drawing a parallel to "breaks" and "bursts" in monsoonal precipitation, it is likely that changing atmospheric patterns would dictate local pollution levels. Therefore, this study's main goal is to identify favorable atmospheric conditions and patterns when high DMO8 values are observed during NAM (i.e., July and August) in the PNA.

Data

Meteorological and air quality data are available for NAM from 2006 to 2016 within the PNA. There were 682 days possible over the study period representing 11 monsoon seasons; however, selection of days for review were limited to those having: 1) at least one DMO8 observation in the PNA, 2) 12Z (0500 LST) and 00Z (1700 LST) rawinsonde profiles (i.e., mandatory levels between surface and 300hPa), and 3) ozone precursor readings, including oxides of nitrogen (Monks et al., 2015) and carbon monoxide (Yamasoe et al., 2015). A modest reduction in potential study days occurred from missing rawinsonde wind observations, primarily in the years 2010 and 2011, compounded by some gaps in daily precursor representation as only days with all 24-hourly observations were analyzed. Consequently, data inclusion restrictions resulted in 509 out of 682 possible days (74.6 percent) for evaluation.

Radiosondes are launched in the Phoenix-Mesa MSA regularly only during the monsoon (i.e., mid-June through late September) by the local water/power utility, Salt River Project, in conjunction with the National Weather Service Forecast Office Phoenix. Location of launch site is centrally located within the PNA in an urbanized area (33.45N, -111.95W) and is close to the Tempe monitor ("TE" in Fig. 3.1). Data are available via the National Oceanic and Atmospheric Administration/Earth System Research Laboratory radiosonde database (ESRL, 2017)

The Phoenix 12Z and 00Z rawinsonde data establishes the vertical atmosphere represented when new daily ozone production begins (i.e., after sunrise) and again near the typical late afternoon peak in ozone concentrations (e.g., Shutters and Balling, 2006). Although the use of an afternoon rawinsonde launch during the monsoon could produce local “convective contamination” concerns (Giaiotti et al., 2007), the local meteorological conditions are specifically required for this study to determine the association with ozone concentrations within the PNA.

Rawinsonde variables considered were geopotential height, temperature, dewpoint, wind speed, and wind direction at the following levels: Surface, 925, 850, 700, 500, 400, and 300 hPa. Three additional variables were derived. First, the parameter “dewpoint depression” was calculated for its relationship to cloud cover approximation (Vasques, 2011), since cloud cover affects solar insolation received at the surface and interferes with the photochemistry necessary for new ozone production (e.g., Wayne, 1987). The second and third derived variables were zonal (U) and meridional (V) wind components to replace and overcome the difficulties in using a single wind direction (0° to 360°) in statistical analyses.

For ozone, DMO8 values were extracted from EPA’s Air Quality System database (EPA, 2017) for the 20 nonattainment ozone monitoring sites sampling in the PNA at the time of this study (tribal monitors were not used). Additionally, “previous day DMO8” values were stored as a separate variable to be tested for significance as an ozone persistence factor. In this study, only the single highest reporting monitor DMO8 value represented the PNA for a given day. Therefore, it’s important to note that spatial characteristics of NAAQS ozone exceedances are beyond the scope of the current research.

Ozone precursor data were collected from the JLG Phoenix Supersite (denoted as "PS" in Fig. 3.1) and like DMO8 values are publicly accessible from U.S. EPA's Air Quality System pollutant database (U.S. EPA, 2017). Location of this monitor is urban and has been used in prior studies to identify ozone and ozone precursor relationships in the PNA (e.g., Shutters and Balling, 2006). Precursors evaluated in this study were the 24-hour arithmetic mean for both carbon monoxide and oxides of nitrogen (i.e., NOx), the latter representing the sum of nitrogen oxide and nitrogen dioxide (e.g., Dunea et al., 2014).

Methods and Results

After data restrictions were implemented, the resultant 509 study days between 2006 and 2016 were stratified into two categories based on the highest reporting DMO8 value within the nonattainment area for a given day. The first grouping of days is comprised of those observations that exceeded the current NAAQS (DMO8 greater than or equal to 71 ppb). This exceedance category is denoted as "EXD" days in this study. The EXDs accounted for 139 days or 27.3% of available study days. The other daily category included all non-exceeding days, labeled as "NEXD" days. The NEXD grouping constituted 370 instances or 72.7% of the record.

Basic univariate statistical analyses showed 80 of the 101 study variables having deviation from normality. Therefore, a Monte Carlo permutation nonparametric two-sample test was employed and indicated statistically significant differences in means between EXD and NEXD days being present to the 0.01 significance level (i.e., *p*-value $\leq$0.01) for 40 atmospheric variables and one pollutant parameter. Interestingly, although the “previous day DM08” variable was found to be significant, both the 24-hour mean NOx and carbon monoxide parameters were not significant to the *p*-value $\leq$0.01, suggesting that day-to-day local precursor emissions in the PNA may be steady in general during NAM and that ozone accumulation causing NAAQS exceedances is dependent on specific atmospheric conditions. Significant atmospheric variables constitute a mix of geopotential height, temperature, wind direction (U and V components), wind speed, and moisture with representation at all mandatory levels found for both the morning (0500 LST) and afternoon (1700 LST) periods.

Compared with NEXD days, morning environments for EXD occurrences are characterized by 1) elevated pressure level heights throughout atmospheric column, 2) deep easterly flow from the surface through 400 hPa, 3) lighter wind speeds aloft at 700 and 300 hPa, 4) warmer PBL temperatures between 925 and 700 hPa, and 5) slightly more humid middle and upper levels from 700-300 hPa (Table 3.1).

Table 3.1
Listing of 12Z (0500 LST) rawinsonde parameters (Phoenix, Arizona) determined to have statistically significant difference in means to 0.01 significance level (i.e., p-value ≤ 0.01) between days when the maximum DMO8 value in the PNA exceeded the NAAQS (EXD) or did not exceed (NEXD). The n-sizes for EXD (NEXD) days were 139 (370). Units for temperature, dewpoint, and dewpoint depression are in °C, ms^{-1} for wind, and meters for geopotential height.

Parameter	95% Confidence Mean Difference (EXD and NEXD)	95% Confidence Mean EXD	95% Confidence Mean NEXD
Surface U Component	0.3 - 1.3	(-2.0) - (-1.2)	(-1.0) - (-0.4)
925 hPa U Component	1.2 - 2.9	(-1.8) - (-0.4)	0.4 - 1.4
850 hPa U Component	1.2 - 2.5	(-0.3) - 0.6	1.6 - 2.4
850 hPa Temperature	0.6 - 1.6	24.5 - 25.4	23.6 - 24.1
700 hPa Wind Speed	0.2 - 1.2	3.9 - 4.7	4.8 - 5.3
700 hPa V Component	0.4 - 1.9	0.3 - 1.6	1.7 - 2.6
700 hPa U Component	1.3 - 2.5	(-1.5) - (-0.5)	0.5 - 1.2
700 hPa Temperature	0.8 - 1.5	12.3 - 12.9	11.3 - 11.6
700 hPa Geopotential Height	5.3 - 13.0	3182.6 - 3189.4	3174.8 - 3178.8
700 hPa Dewpoint Depression	0.8 - 3.1	8.3 - 10.4	6.8 - 7.8
500 hPa U Component	1.6 - 3.8	(-2.6) - (-0.8)	0.4 - 1.6
500 hPa Geopotential Height	8.8 - 18.7	5906.6 - 5915.1	5894.4 - 5899.6
500 hPa Dewpoint	1.4 - 5.5	(-17.0) - (-13.7)	(-20.0) - (-17.6)
500 hPa Dewpoint Depression	1.4 - 5.5	7.2 - 10.6	11.1 - 13.5
400 hPa U Component	2.9 - 5.1	(-1.5) - 0.3	2.8 - 4.0
400 hPa Geopotential Height	9.0 - 19.5	7617.4 - 7626.2	7604.4 - 7610.3
400 hPa Dewpoint	2.1 - 6.4	(-32.4) - (-28.6)	(-36.0) - (-33.6)
400 hPa Dewpoint Depression	2.0 - 6.4	11.7 - 15.5	16.7 - 19.0
300 hPa Wind Speed	1.3 - 3.2	8.11 - 9.6	10.5 - 11.8
300 hPa U Component	3.7 - 6.4	0.1 - 2.5	5.6 - 7.1
300 hPa Geopotential Height	9.0 - 21.4	9713.4 - 9723.4	9699.3 - 9707.0
300 hPa Dewpoint Depression	2.0 - 5.6	11.4 - 14.5	15.8 - 17.7
300 Dewpoint	2.0 - 5.6	(-46.5) - (-43.4)	(-49.8) - (-47.8)

By the late afternoon, moisture parameters lose significance in relating to ozone exceedances, yet, 1) geopotential heights remain relatively high, 2) PBL temperature stays warmer, and 3) lighter winds persist at 700 and 300 hPa. Additionally, 4) lighter winds nearer to the surface at 925 and 850 hPa also become significant. Another key difference is 5) flows aloft at 500 and 400 hPa still tend to hold an easterly direction; however, in the PBL only the 700 hPa pressure level continues to be statistically significant and maintains a negative U component through the day when DMO8 values reached unhealthy levels (Table 3.2).

Table 3.2
Listing of 00Z (1700 LST) rawinsonde parameters (Phoenix, Arizona) determined to have statistically significant difference in means to 0.01 significance level (i.e., *p*-value ≤0.01) between days when the maximum DMO8 value in the PNA exceeded the NAAQS (EXD) or did not exceed (NEXD). The *n*-sizes for EXD (NEXD) days were 139 (370). Units for temperature, dewpoint, and dewpoint depression are in °C, ms^{-1} for wind, and meters for geopotential height.

Parameter	95% Confidence Mean Difference (EXD and NEXD)	95% Confidence Mean EXD	95% Confidence Mean NEXD
Surface Temperature	1.1 - 2.1	40.0 - 40.8	38.4 - 39.1
925 hPa Wind Speed	0.3 - 1.2	3.6 - 4.3	4.5 - 5.0
925 hPa Temperature	0.9 - 1.9	34.5 - 35.3	33.2 - 33.8
850 hPa Wind Speed	0.6 - 1.3	3.2 - 3.8	4.3 - 4.7
850 hPa U Component	0.3 - 1.2	2.3 - 3.0	3.1 - 3.7
850 hPa Temperature	0.8 - 1.8	27.3- 28.1	26.1 - 26.7
700 hPa Wind Speed	0.2 - 1.2	3.6 - 4.5	4.5 - 5.1
700 hPa U Component	1.4 - 2.8	(-1.3) - (-0.1)	0.9 - 1.7
700 hPa Temperature	0.8 - 1.5	13.3 - 13.9	12.2 - 12.6
700 hPa Geopotential Height	3.0 - 10.8	3184.8 - 3191.4	3179.0 - 3183.3
500 hPa U Component	1.6 - 3.6	(-2.6) - (-0.9)	0.3 - 1.3
500 hPa Geopotential Height	7.2 - 17.5	5915.6 - 5924.3	5904.7 - 5910.3
400 hPa U Component	2.2 - 4.5	(-1.5) - 0.4	2.2 - 3.4
400 hPa Geopotential Height	7.0 - 18.0	7629.8 - 7639.1	7618.9 - 7625.1
300 hPa Wind Speed	1.3 - 3.4	8.1 - 9.8	10.7 - 12.0
300 hPa U Component	2.9 - 5.7	0.0 - 2.4	4.7 - 6.3
300 hPa Geopotential Height	8.0 - 20.9	9730.5 - 9741.1	9717.5 - 9725.4

The persistence of an easterly flow for the EXD group is an intriguing finding. The 700 hPa level would correspond to Phoenix's summertime upper PBL (approximately 3000 meters) (Lee and Fernando, 2013). The consequence of a stable atmosphere with light easterly flow near 700hPa could very well be significant by not allowing ozone aloft in the upper mixed layer to disperse downwind of the city with prevailing westerly mountain-valley winds during the daytime. Consequently, it is proposed in this study that "damming" of vertically mixed ozone from a blocking 700 hPa flow occurring over reduced afternoon near-surface winds (i.e., 925 and 850 hPa) may aid in creating an ozone-rich nocturnal residual layer over the PNA. The fumigation of an aged ozone air mass aloft adding to a newly forming ground-level ozone is not novel and has already been thought to be significant for higher ozone concentrations for Phoenix (Lee and Fernando, 2013) and other rural locations in the southwest U.S. (e.g., VanCuren, 2015). This study does provide a synoptic setup that may be ideal for such ozone fumigation contribution toward ozone accumulation in the PNA.

Furthermore, the previous day DMO8 mean parameter is statistically significant on the order of 6.7 to 10.2 ppb higher (95% confidence interval) for NAAQS exceeding days than non-exceeding days, while actual mean values were 70.9 ppb versus 62.4 ppb, respectively. Since the mean previous day DMO8 value is very near the NAAQS, it is reasonable to believe that ozone air quality events in the PNA could be episodic in nature with identified atmospheric conditions in this study conducive for unhealthy ozone likely capable of lasting over the region multiple days at time. However, further discussion on potential longevity of ozone exceedances are not expounded upon in this study.

Principle Components Analysis (PCA) was next used to identify underlying relationships and explained variance between the 41 variables to find what parameters may be better predictors for EXD versus NEXD days (Davis, 1986; Wilks, 2011). The analysis created a correlation matrix to group the 41 variables into eigenvectors or components that have high multicollinearity. The resultant eigenvalues reveal the percent variance explained. For this study, the first three components explained 54.7% of the total variance and were considered distinctive from other components by using PCA scree plot and broken stick model methods. It is accepted, although with some subjectivity, that components can be considered insignificant along a level scree plot slope curve with low eigenvalue variance contributions and for when components fall below the broken stick model curve (Jackson, 1993).

Largest PCA loading values in the first component (PC 1) correspond to daily geopotential heights and wind direction in the middle and upper levels of the atmosphere (500-300 hPa). Conceptually, PC 1 might be termed as a "monsoon ridge strength and position" (MRSP) factor. The second component (PC 2) is dominated by middle and upper level moisture (700-300 hPa) in the morning hours having a negative relationship with afternoon PBL temperatures. Therefore, PC 2 can be defined as a "solar radiation availability" (SRA) variable. Principal component three (PC 3) has prominent easterly flow within the PBL tied with reduced wind speeds in general. Therefore, PC 3 might be termed "planetary boundary layer dispersion" (PBLD).

To better determine if the three PCA factors are linked with daily PNA ozone concentrations PCA daily parameter scores for the three components retained were used as inputs for Linear Discriminant Analysis (Wilks, 2011). The analysis assesses predictive power for correctly classifying ozone exceedance days versus non-exceedance days. After a cross validation check was applied to account for the use of the same dataset from which the PCA scores were derived, overall correct daily categorical prediction (EXD and NEXD) remained at 73.3 percent (373 of 509 study days). Specifically, the EXD category was classified accurately 74.8 percent (104 out of 139 days) and NEXD days 72.7 percent (269 out of 370 days), respectively.

Mean synoptic weather patterns linked to correctly classified and misclassified EXD and NEXD days are next presented using the "daily composite" feature of the high-resolution North American Regional Reanalysis (NARR) dataset that generates mean synoptic pattern plots based on user specified dates (Mesinger et al., 2006). Input variables to create mean synoptic patterns were chosen that helped summarize the key distinctions determined to exist between the EXD and NEXD groups. Explicitly, they are the 1) 500 hPa geopotential height and flow (Fig. 3.3) and 2) 700 hPa vector wind (Fig. 3.4). Dimensions for maps depicted in Figures 3.3 and 3.4 were bounded between 27N and 42N latitude and 100W to 125W longitude. This restriction shows the region generally affected by NAM (Adams and Comrie, 1997).

Mean 500 hPa synoptic plots are shown in Fig. 3.3. The analysis for correctly classified EXDs indicates an amplified ridge occupying the western U.S. with a strong anticyclone (i.e., ≥5940 meters) centered over the Four Corners region and easterly flow affecting the PNA (Fig. 3.3a), while for NEXDs the ridge strength is weaker (i.e., ≤5920 meters) and suppressed in latitude forcing southwest flow over the PNA due to low-pressure troughing off the West Coast U.S. (Fig. 3.3b). Alternatively, exceedance and non-exceedances of the NAAQS have also occurred less frequently under mean 500 hPa patterns shown in Figs. 3.3c and 3.3d, respectively, which resemble possible transitions of the more common EXD and NEXD synoptic setups based on strength and positioning of the monsoon circulation.

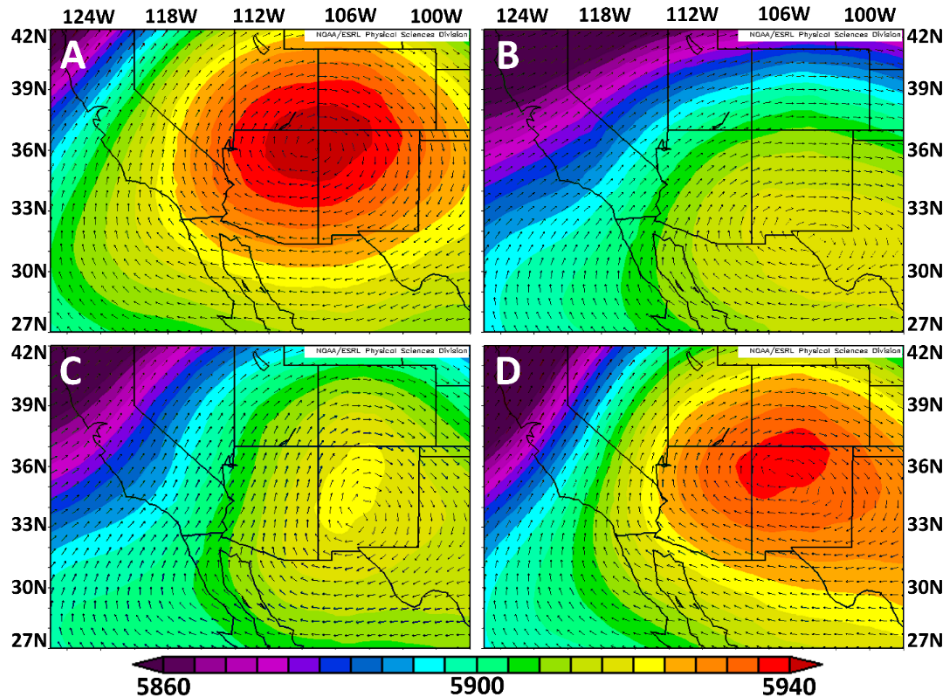

Fig. 3.3. Daily composite maps showing mean 500 hPa height (meters) and synoptic flow patterns for correctly classified EXDs (104 days) (A), correctly classified NEXDs (268 days) (B), misclassified EXDs (35 days) (C), and misclassified NEXDs (102 days) (D). For reference, the Phoenix rawinsonde launch site within the PNA is located at 33.45N, 111.95W. Images created by the National Oceanic and Atmospheric Association/Earth Systems Research Laboratory Physical Science Division, Boulder, Colorado (2018).

Complimenting mean 500 hPa patterns shown in Fig. 3.3 are corresponding mean analyses at the 700 hPa level (Fig. 3.4). The EXD group in Fig. 3.4a has light easterly flow over central Arizona (≤ 2 ms^{-1}) compared to faster southwesterly winds (≥ 3 ms^{-1}) in the majority of NEXD days (Fig. 3.4b). The misclassified EXD group (Fig. 3.4c) deviates from the larger EXD group by having light southerly, instead of light easterly, flow. Given the topographic configuration in central and southern Arizona, early afternoon monsoon thunderstorm activity developing over higher terrain north, east, and southeast of Phoenix is less likely to propagate into the PNA to interfere with local ozone production and accumulation with this secondary EXD pattern (Wallace et al., 1999).

The mean 700 hPa pattern for misclassified NEXD days (Fig. 3.4d) is an established yet modest regional southeasterly flow (≤3 ms^{-1}) versus stronger southwesterly flow in the more common West Coast trough NEXD setup (Fig. 3.4b). Moist southeasterly flow tends to be associated with active monsoon days in Arizona and is even a characteristic of an identified severe thunderstorm pattern for central Arizona, which would include the PNA (Maddox et al., 1995). This secondary NEXD scenario can bring widespread convection and gusty outflow wind boundary passages for local pollutant dispersion, along with excessive convective debris cloud cover from even distant thunderstorm complexes when upper level steering winds spread anvil clouds northwestward over the lower elevations, which would likely limit new ozone production (e.g., Wayne, 1987).

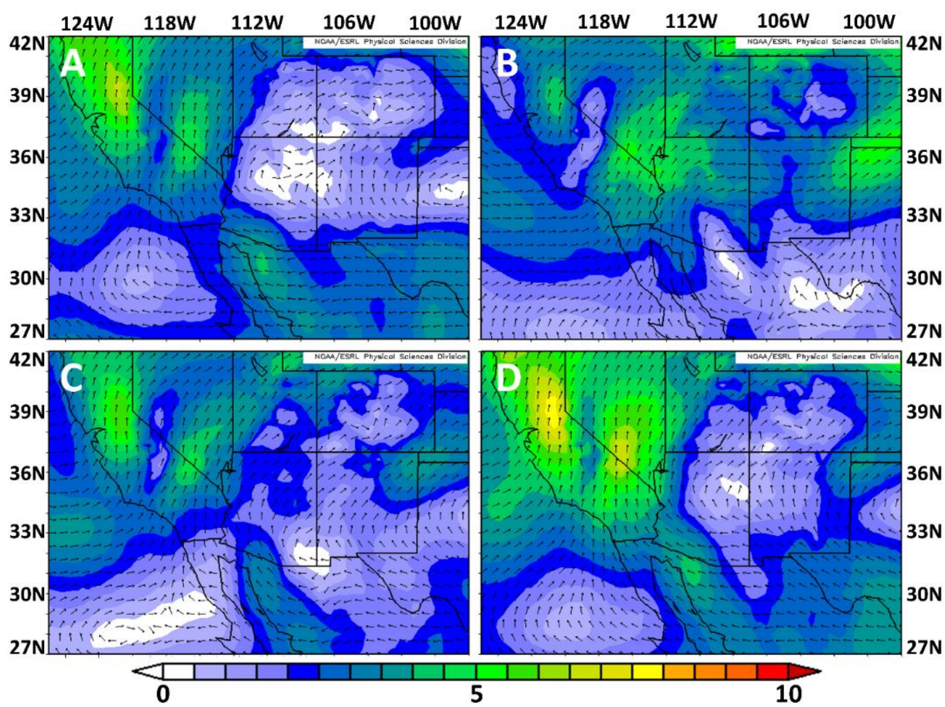

Fig. 3.4. Daily composite maps showing mean 700 hPa vector wind (ms^{-1}) for correctly classified EXDs (104 days) (A), correctly classified NEXDs (268 days) (B), misclassified EXDs (35 days) (C), and misclassified NEXDs (102 days) (D). For reference, the Phoenix rawinsonde launch site within the PNA is located at 33.45N, 111.95W. Images

created by the National Oceanic and Atmospheric Association/Earth Systems Research Laboratory Physical Science Division, Boulder, Colorado (2018).

Conclusions

This study has investigated the degree to which surface and upper atmospheric variables corresponded to DMO8 values observed in the PNA during the monsoon season (i.e., July and August) from 2006 to 2016. Additionally, primary and secondary synoptic patterns representing EXDs and NEXDs were determined. Ultimately, surface ozone concentrations in the PNA are found to be heavily influenced by the evolution of the monsoon circulation and repeating nature of two particular synoptic configurations over the southwest U.S.

Synoptic characteristics distinguishing the majority of EXD and NEXD days are related to the strength and positioning of the monsoon ridge impacting atmospheric dispersion within the PBL. For most EXDs, a strong anticyclone positioned near the Four Corners region creates a persistent and light easterly blocking flow at 700 hPa, countering typical westerly mountain-valley daytime winds. The primary EXD pattern also brings relatively light 925 and 850 hPa winds to limit pollutant dispersal. Conversely, a majority of NEXD days have deep southwesterly flow from West Coast U.S. troughing aligning with the local daytime mountain-valley circulation to reduce ozone accumulation in the PNA.

A secondary synoptic pattern accounting for nearly a quarter of NEXD days was also identified and is likely a transition of the monsoon circulation between the primary EXD and NEXD patterns. The significance of the NEXD secondary scenario is that it represents a known setup for active and widespread convective storm activity near the PNA due to a predominant moist southeast flow into central Arizona.

Collectively, these findings will help our understanding of NAM's influence on summer ozone concentrations for the Phoenix metropolitan area.

CHAPTER 4

VERTICAL SOUNDING PARAMETER ALIGNMENTS DICTATING OZONE LEVELS IN PHOENIX, ARIZONA DURING THE MONSOON

This chapter identifies common atmospheric sounding configurations favorable for healthy and unhealthy ozone concentrations observed in the U.S. Environmental Protection Agency declared Phoenix Nonattainment Area between 2006 and 2017. A version of this chapter titled: "Atmospheric composite sounding analysis as a forecasting tool for ozone accumulation in a semi-arid metropolitan area during the North America Monsoon: Phoenix, Arizona" is under revision with the journal *Weather and Forecasting*. This article was coauthored with Randall S. Cerveny.

Abstract

Phoenix, Arizona, observes a high summertime frequency for daily maximum 8-hour ozone averages (DMO8) exceeding 70 parts per billion, resulting in nonattainment status by the U.S. Environmental Protection Agency (U.S. EPA). Public warning of air quality episodes is complicated during the July-August period by the dynamic nature of the North American Monsoon. This study discusses the use of composite atmospheric sounding analysis (constructing average sounding conditions for specific recurring events) to forecast Air Quality Index ozone classifications of Good (GD), Moderate (MD), and collectively categories exceeding the 2015 ozone standard (EXD) for the monsoon. Composite sounding analysis, using the Phoenix 12Z (0500 LST) rawinsonde data (2006-2017), identifies "pollutant dispersion windows" for ozone accumulation or dispersal (i.e., EXD or GD events, respectively) for Phoenix. A favorable EXD atmosphere is associated with a “Four Corners High” synoptic pattern bringing relatively light winds at and below 700 hPa (≤4.5 ms^{-1}) and higher easterly winds above (≤12.3 ms^{-1}). Healthy ozone days (GD) are a function of Pacific troughing forcing westerly wind alignments above the surface reaching 6.7 (19.5) ms^{-1} by 700 (200) hPa. Surprisingly, large standard deviations over 10°C for dewpoint temperature at midlevels (500-400 hPa) were determined for GD, MD, and EXD ranges. Additionally, modest temperature deviations and mean differences are noted at significant pressure levels. Consequently, wind speed and direction are better indicators when forecasting ozone accumulation potential. These results are pertinent to air quality meteorologists responsible for disseminating ozone forecasts for heavily urbanized areas of the U.S. Southwest.

Introduction

Tropospheric ozone poses a risk to both human health (Gold et al., 1996; Owens, 2017) and vegetation (Mills et al., 2006). The formation of ozone is derived through complex photochemical chemical reactions primarily between sunlight, oxygen, oxides of nitrogen, and volatile organic compounds (Quincey et al., 2007; Wayne, 1987). Phoenix, Arizona, has been shown to be susceptible to recurring ozone levels reaching unhealthful levels based on U.S. Environmental Protection Agency (U.S. EPA) pollutant standards (Malloy, 2018). Consequently, the Phoenix mean statistical area (MSA) represents a designated nonattainment area for ozone, specifically concerning the daily maximum 8-hour average (DMO8) (Fig. 4.1a). The MSA populace has nearly five million residents as of 2017 (U.S. Census Bureau, 2018) making it the eleventh most populated metropolitan area in the United States. This represents a significant population at risk for health effects due excessive ozone concentration exposure.

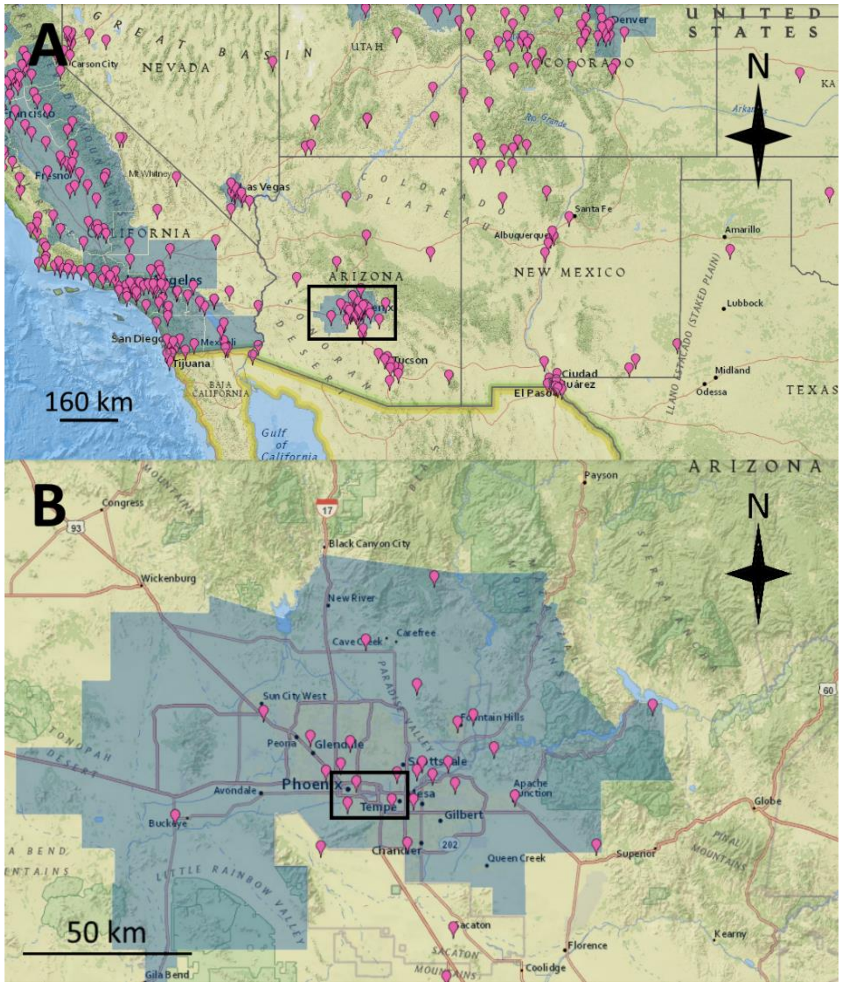

Fig. 4.1. U.S. Southwest study area (A). Large black box contains Phoenix Mean Statistical Area and ozone nonattainment area (grey shade). Balloon icons represent active ozone monitoring stations in region. Zoom in of ozone nonattainment area and local topography of Phoenix are shown (B). Small black box indicates Phoenix sounding launch location (specifically, 33.45°N, 111.95°W). Map details provided by U.S. EPA's AirData App website (U.S. EPA, 2018).

The Phoenix Nonattainment Area (termed PNA in this study) is spatially large, encompassing an area of nearly 13,000 km^2. The PNA is best described as a mixed land use including urban, suburban, and rural zones. The most urbanized area of the PNA is the central business district of Phoenix in south-central portions of the PNA. The current ozone monitoring network includes 26 monitoring sites that are maintained by state, local, and tribal air regulatory agencies (Fig. 4.1b).

Ozone pollutant dispersion patterns over the PNA are heavily dictated by the existence of a prominent topographically-induced mountain-valley circulation (Malloy 2018). As noted in Fig. 4.1, the north and east boundaries of the PNA represent a transition from a lower valley toward desert foothills and finally significant terrain in excess of 1,500 meters. The close proximity of nearby higher topography versus the lower elevations of downtown Phoenix (i.e., approximately 380 meters elevation) creates a recurring mountain-valley circulation that has been found to be an important factor affecting local diurnal trends in pollution levels (e.g., Ellis et al., 1999; Fast et al., 2000; Lee and Fernando, 2013).

On a seasonal basis, the PNA has a high propensity to record elevated surface ozone concentrations during the summer months. During that time of year, the position of the PNA in the northern Sonoran Desert also makes the area subject to influences by the summer North American Monsoon (NAM). The NAM is a large-scale atmospheric circulation phenomenon affecting primarily the U.S. Southwest and northern Mexico (Adams and Comrie, 1997; Douglas et al., 1993). The NAM is characterized by 1) atmospheric instability (Diem and Brown, 2009; Heinselman and Schultz, 2006), 2) intermittent rainfall (Carleton, 1986; Mullen et al., 1998), 3) severe weather hazards (Brazel and Nickling, 1986; King and Balling, 1994; Maddox et al., 1995), and 4) varying levels of atmospheric dispersion affecting pollutant buildup potential, including ozone accumulation (e.g., Ellis et al., 2000; Malloy, 2018; Shi et al., 2012).

A previous study (Malloy, 2018) statistically identified a variety of temperature, moisture, and wind related meteorological parameters between the surface and 300 hPa. Variations in those parameters were found to be statistically significant in their association with days when the DMO8 value in the PNA exceeded the 2015 U.S. EPA standard of 70 parts per billion (ppb) during the months of July and August. Although the Malloy (2018) results were useful in identifying specific thresholds for a range of sounding parameters associated with exceeding days, that study did not explicitly address how significant sounding parameters may be working in concert in reference to daily DMO8 variability, or in other words, it failed to identify the common or average sounding associated with ozone exceedances. This is important in an operational forecasting framework in that leveraging single parameters without context to the overall environment may result in biased and inaccurate forecasts.

Therefore, the intention of this study is to use a rawinsonde composite analysis approach for establishing differences in temperature, moisture, and wind characteristics that have preceded ozone exceedance and non-exceedance situations. The study's fundamental goal is to determine the sounding signatures for the planetary boundary layer (PBL), as well as upper levels, for ozone exceedance days (i.e., DMO8 value ≥70 parts per billion). To do so, data collected includes the morning vertical environment (12Zor 0500 LST) before peak ozone production in the PNA, which typically occurs in the afternoon hours (e.g., Atkinson-Palombo et al., 2006).

The technique of composite analysis is both viable and accepted in the scientific community for identification of vertical atmospheric variables associated with specific meteorological events, dating back to initial tornado forecasting analyses (Fawbush et al., 1951). More recently, for example, Rodrigues and colleagues (2010) investigated mean differences in sounding parameters between thunderstorm and non-thunderstorm days in Sao Paulo, Brazil, while Schrage et al. (2007) employed composite sounding analysis to determine cloudiness potential during the West African Monsoon. Other examples of employing the technique include identifying vertical profile characteristics favoring fog versus non-fog days in northeastern Japan (Sugimoto et al., 2013) and identifying atmospheric conditions preceding severe hail reports in northern Arizona during the NAM (Malloy, 2011).

Specific to this study, the method of composite sounding analysis is applied to morning environmental conditions, taken over the PNA area during the NAM, to establish differences between observed exceeding versus non-exceeding DMO8 levels (termed EXD and NEXD, respectively). The period under review is for the months of July and August between 2006 and 2017.

Data

Phoenix Rawinsonde

The North American Monsoon (NAM) officially begins on June 15 and concludes on September 30. The study period for this research, however, is restricted to the months of July and August for two major reasons. First, although the NAM may develop early in June and linger into the month of September (Adams and Comrie, 1997), historical interseasonal variability for an established monsoon pattern has been shown to be higher for what could be considered the transition months for the onset (June) and breakdown (September) (e.g., Ellis et al., 2004). Second, Phoenix rawinsonde data (12Z and 00Z) are made intermittently through a collaborative effort between the local power-utility company Salt River Project and the National Weather Service Office Phoenix. Location of launches have been consistent from year-to-year within the PNA (see Fig. 4.1b), yet focus for rawinsonde releases are almost exclusively reserved for the NAM with greatest record availability during the months of July and August. Inclusion of the transition months having relatively limited sample sizes are likely to bias composite type analyses and comparisons.

Furthermore, for this study, rawinsonde data were limited to 12Z (0500 LST) since the aim of the study is establishing common NAM morning vertical profiles before DMO8 exceedances would typically occur in the PNA (e.g., Ellis et al., 1999) for potential use in forecasting unhealthy ozone days. There were no restrictions given on exporting the sounding parameters of pressure height, temperature, dewpoint, wind speed, and wind direction for any specific pressure levels. Complete Phoenix daily soundings totaled 731 out of a possible 744 (98.2 percent) and were made available by the NOAA/ESRL Radiosonde Database (NOAA/ESRL, 2018).

Phoenix DMO8 Values

DMO8 value selection for the study period was limited to the 26 currently active PNA ozone monitoring sites (as of August, 2018) (see Fig. 4.1b) via EPA's Air Quality System (U.S. EPA, 2018). All 731 days (limited by rawinsonde data availability) had at least one valid PNA DMO8 value. Of those days, 206 days were classified as exceedances and 537 were classified as non-exceedance for the 12 monsoon seasons. However, rawinsonde data gaps allowed only 203 of 206 EXD (98.5 percent) and 528 of

538 (98.3 percent) NEXD to be evaluated with a corresponding 1200 UTC sounding. Effects of this reduction in data should be negligible due to a vast majority of respective EXD and NEXD days still being included for review.

Methods

The 12Z rawinsonde measurements were aggregated into mean values to establish the morning temperature, moisture, and wind variability for exceedance (EXD) and non-exceedance (NEXD) days. Furthermore, the NEXD day group is subdivided based on the following U.S. EPA's Air Quality Index (AQI) categorical schema (U.S. EPA Ozone, 2018): "Good" (0-54 ppb) and "Moderate" (55-70 ppb). According to the U.S. EPA, the Moderate AQI range "marks the level above which EPA begins cautioning at-risk groups" (U.S. EPA Ozone, 2018). Therefore, days with this range should be considered for evaluation independent of the Good AQI category.

No subdivision was given to the EXD group, which for the purpose of this study, encompassed all AQI categories representing DMO8 values over the 70 ppb exceedance standard. Those AQI categories and ppb ranges are as follows: "Unhealthy for Sensitive Groups" (71-85 ppb), "Unhealthy" (86-105), "Very Unhealthy" (106-200), and "Hazardous" (≥201 ppb). Applying the 2015 U.S. EPA standard retroactively to the study period of 2006 to 2017, the highest DMO8 AQI category reached at Phoenix would have been "Unhealthy" with a measurement of 96 ppb occurring twice (17 and 19 July, 2006). Such high concentrations were rare considering the large sample size for EXD versus only ten occurrences over the study period. The resultant distribution of Good (GD), Moderate (MD), and EXD days for PNA are 203, 444, and 84, respectively. A total of nine MD days and one GD day were not included in the evaluation due to rawinsonde unavailability. Composites were created for the three groupings using the merging capability of the Universal RAwindsonde Observation software program (RAOB, 2018). The program's merge option retains all data and interpolates data for standard significant pressure levels only if missing values are present.

To add context for the soundings with associated larger scale NAM patterns, mean daily 500 hPa geopotential height and 700 hPa vector wind synoptic plots are constructed for each of the three DMO8 groupings via the widely utilized North American Regional Reanalysis (NARR) dataset intended for research purposes (Mesinger et al., 2004). The 500 hPa height pattern is often relied upon to track the strength and position of the NAM circulation (Adams and Comrie, 1997), while the 700 hPa level represents the potential upper extension of the planetary boundary layer (PBL) in the desert areas of the U.S. Southwest during the summer months (Lee and Fernando, 2013).

Results and Discussion

Phoenix Ozone Exceedances

There exists wide variability in the morning vertical atmospheric conditions preceding observed DMO8 exceedances in the Phoenix Nonattainment Area, especially considering midlevel moisture and upper level wind speed (Table 4.1). Specifically, standard deviations for dewpoint temperatures were 11.7°C at 400 hPa and were no less than 4.1°C within the PBL. Wind speed standard deviations were less and ranged between a minimum of 1.5 ms^{-1} at the surface to near 6.3 ms^{-1} at the 200 hPa pressure level. However, temperatures in the atmospheric column preceding ozone exceedances exhibited much less deviance; ranging only 1.3°C to 2.6 °C at any significant pressure level height between the surface and 100 hPa.

Table 4.1
Phoenix, Arizona, 12Z composited sounding mean and standard deviations for temperature, dewpoint, and wind speed at significant pressure levels associated with ozone exceedance days. Units for pressure are hectopascals (hPa), temperature and dewpoint are °C, and ms^{-1} for wind speed.

Pressure	Temperature		Dewpoint		Wind Speed	
	Mean	Std. Dev.	Mean	Std. Dev.	Mean	Std. Dev.
100	-71.1	2.3	-85.1	2.5	6.8	3.2
150	-64.6	1.9	-78.4	4.1	11.1	6.1
200	-52.9	1.6	-67.7	6.5	12.3	6.3
250	-41.6	1.3	-56.4	8.5	10.2	5.6
300	-31.9	1.5	-46.6	10.4	8.6	4.6
400	-16.9	1.4	-31.2	11.7	6.9	3.6
500	-6.5	1.2	-15.6	10.1	6.5	3.5
700	12.7	1.8	3.3	5	4.5	2.5
850	25.1	2.6	9.7	4.5	4.3	2.7
925	29.4	3	12.8	4.8	4.5	2.9
966(Surface)	29.3	2.3	15.7	4.1	2.7	1.5

Atmospheric variability during NAM supporting ozone accumulation in the PNA is demonstrated visually by the large standard deviation ranges for dewpoint at the significant pressure levels (Fig. 4.2a) and the numerous observed profile configurations seen by the “spaghetti plot” for the 203 composited EXD days (Fig. 4.2b).

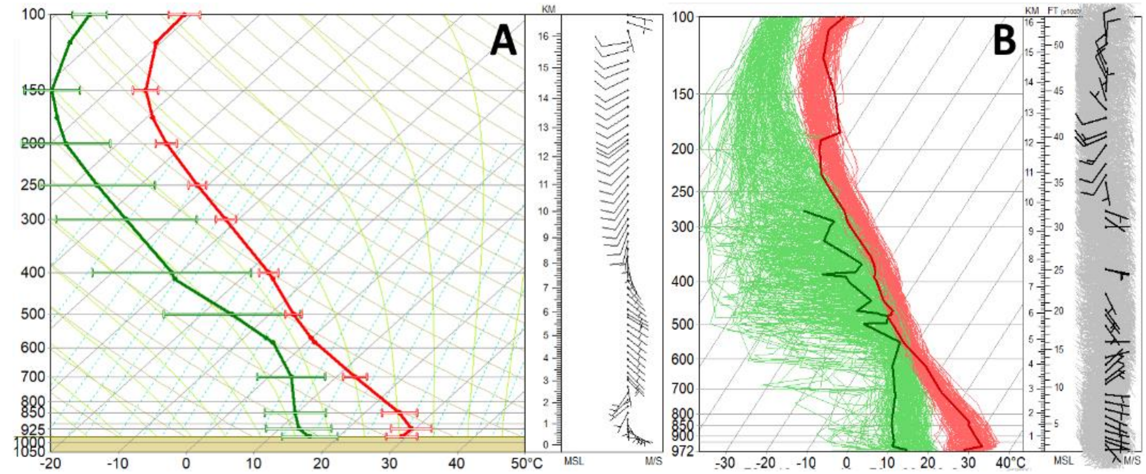

Fig. 4.2. Mean 12Z composite sounding for Phoenix ozone exceedance days (203) (A). Standard deviation error bars at significant pressure levels are plotted for both the dewpoint (green) and temperature (red) mean profiles. Mean atmospheric wind speed and directions are shown on right. Panel B shows spaghetti plot of composited days with bold dewpoint, temperature, and wind corresponding to the sounding with greatest DMO8 concentration observed (19 July 2006; 96 ppb). Units for dewpoint and temperature are in °C, ms^{-1} for wind speed, and hectopascals (hPa) for pressure height.

The greatest DMO8 value recorded in the PNA over the study period was 96 ppb achieved on both 17 and 19 July 2006. The 19 July 2006 profile is highlighted in Fig. 4.2b to showcase an EXD instance. This date was the sixth straight day reaching exceedance values that began on 14 July 2006. The EXD event continued through 26 July 2006, making the entire period a 13-day air quality episode and the longest consecutive EXD day streak in the study period. Fortunately, with regard to health concerns, such long duration air quality episodes are rare, with a majority of exceedance events being only one or two days in length (Fig. 4.3).

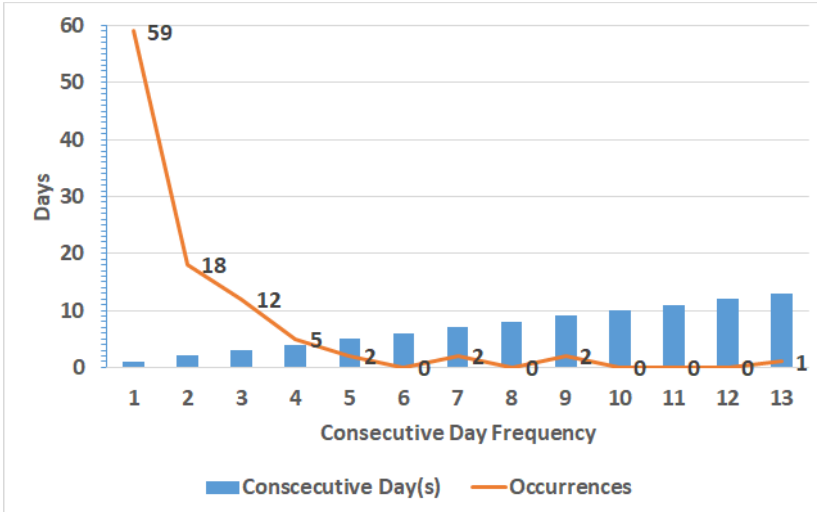

Fig. 4.3. Ozone exceedance day episode duration frequency for the Phoenix Nonattainment Area during the months of July and August (2006-2017).

Key features of the 19 July 2006 morning sounding profile include: 1) a warm and dry inversion near the surface, 2) light easterly to southeasterly flow in the PBL (sub-700 hPa), and 3) cloud cover potential near 500 hPa pressure level based on low dewpoint depression values. Otherwise, light winds throughout the column dominated between the surface and 400 hPa (≤5 ms^{-1}). However, this particular profile should not be considered the only ozone exceedance environment for the PNA given the differences in soundings found for the collective EXD group, especially when considering the variability in vertical profiles throughout the air quality episode noted previously (Fig. 4.4).

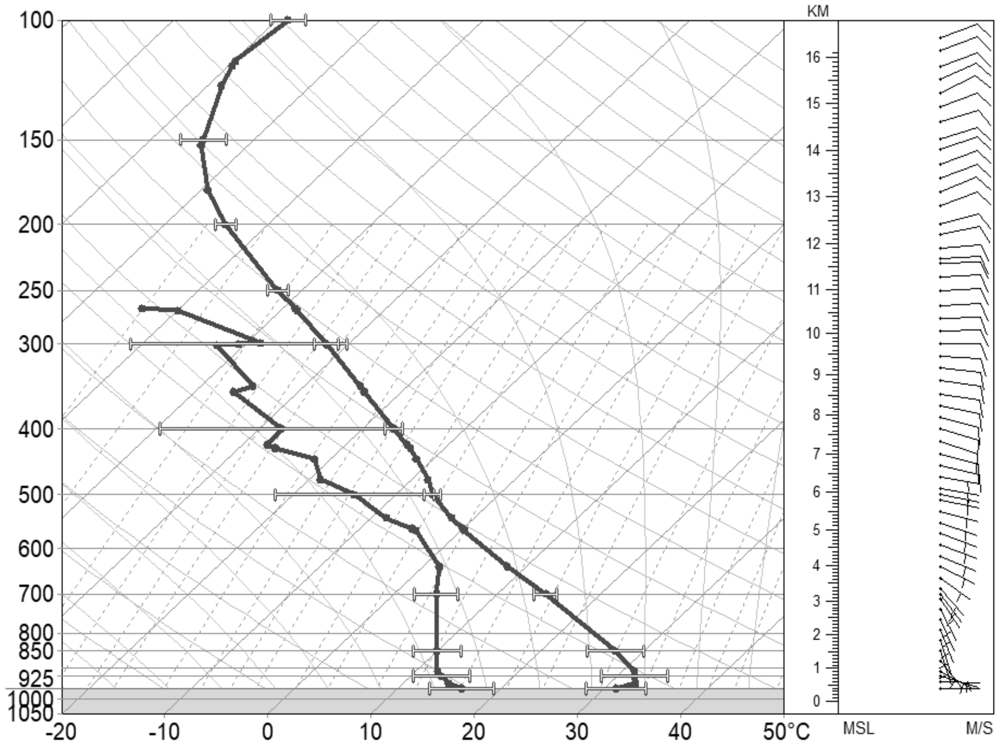

Fig. 4.4. Mean 12Z composite sounding for longest Phoenix ozone exceedance air quality episode (14-26 July 2006) during the months of July and August (2006-2017). Units for dewpoint and temperature are in °C, ms^{-1} for wind speed, and hectopascals (hPa) for pressure height.

It is also important to note that both saturated and unsaturated conditions have preceded DMO8 exceedances. The study area's high day-to-day variability in atmospheric moisture readings during the July and August monsoon period is not a surprising finding. Intraseasonality differences for moisture affecting rain and cloud cover has been well-documented for the North American Monsoon (e.g., Carleton, 1986; Heinselman and Schultz, 2006). What is more important in this finding is that unhealthful DMO8 values may be independent of ambient moisture readings. For instance, although excessive moisture leading to clouds would interrupt the photochemical process necessary for new ozone formation (Wayne, 1987), cloudiness does not preclude higher ozone concentrations already in the region. In the absence of cloud cover, elevated moisture in the PBL may act to limit vertical mixing due to a more homogeneous profile allowing local ozone production to accumulate. Additionally, ozone is not removed directly by rainfall should adequate moisture and instability exist (e.g., U.S. EPA, 2003).

In contrast to a moist environment, an unsaturated profile promotes ultraviolet light to reach the surface and support photochemistry of new ozone formation (Wayne, 1987), while increased insolation also encourages deep vertical mixing and fumigation of aged ozone aloft toward the surface. Although moisture is noted to be quite variable, it is apparent that for the composited EXD group there is an inclination toward a light wind regime (generally under 5 ms^{-1}) below 500 hPa with veering winds between the surface and 850 hPa, then abrupt change to backing winds through 500 hPa (Fig. 4.2a).

Phoenix Ozone Moderate AQI Days

Similar to the EXD group there is no single ideal 12Z atmospheric profile indicative of a Moderate AQI ozone day (MD) given the amount of combinations for temperature, moisture, and wind that existed for the 444 days. Midlevel moisture near 500 hPa and wind speeds aloft near 200 hPa exhibited the greatest variation having large standard deviations up to 12.1°C and 7.8 ms^{-1}, respectively (Table 4.2).

Table 4.2
Phoenix, Arizona, 12Z composited sounding mean and standard deviations for temperature, dewpoint, and wind speed at significant pressure levels associated with ozone Moderate Air Quality Index days. Units for pressure are hectopascals (hPa), temperature and dewpoint are °C, and ms^{-1} for wind speed.

Pressure	Temperature		Dewpoint		Wind Speed	
	Mean	Std. Dev.	Mean	Std. Dev.	Mean	Std. Dev.
100	-70.7	2.3	-85.1	2.5	6.7	3.3
150	-64.7	1.8	-78.5	4.1	13.7	6.8
200	-52.6	1.4	-67.2	7	15.8	7.8
250	-41.4	1.6	-57.3	9.3	13.2	6.9
300	-31.8	1.7	-49.5	10.5	10.6	5.9
400	-16.8	1.6	-35.7	12.1	7.6	4.2
500	-6.4	1.4	-18.8	12	6.5	3.5
700	11.7	1.7	4	4.5	5.0	2.8
850	24.1	2.4	9.5	5.4	4.5	2.5
925	28.8	2.6	12.3	5.6	4.6	2.8
966(Surface)	28.8	2.1	15.1	4.5	2.7	1.8

Once again, temperature at all significant levels showed little variability. Throughout the vertical column a temperature deviation of no more than 2.6°C (925 hPa) was noted. Overall, the PBL did demonstrate the greatest variability in temperature. In similar fashion to Fig. 4.2, the composited sounding for the 444 MD is shown with standard deviation bars (Fig. 4.5a) along with the ensemble of all MD used in the study (Fig. 4.5b).

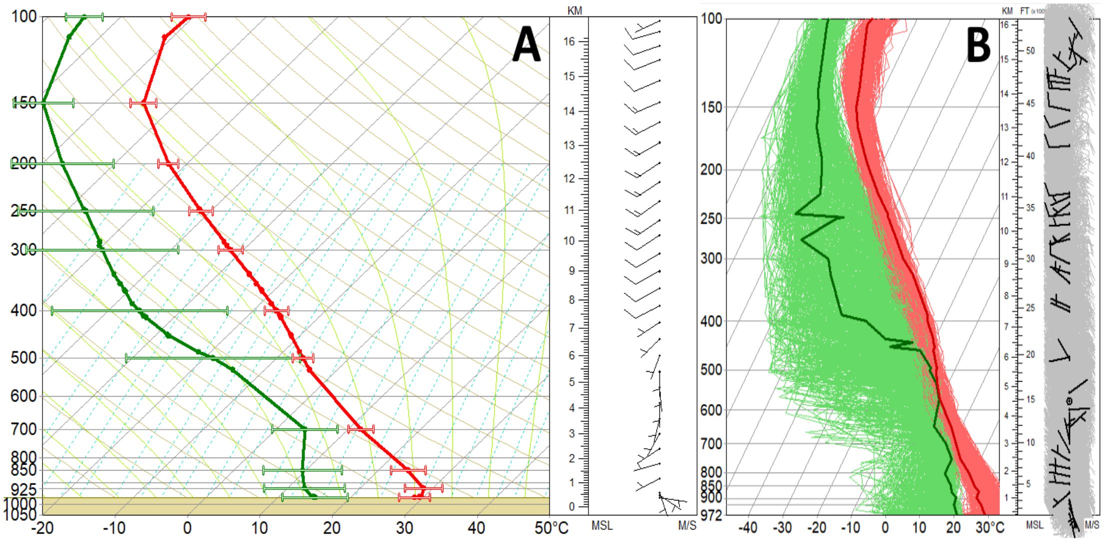

Fig. 4.5. Mean 1200 UTC composite sounding for Phoenix ozone Moderate Air Quality Index (AQI) days (444) (A). Standard deviation bars at significant pressure levels are plotted for both the dewpoint (green) and temperature (red) mean profiles. Mean atmospheric wind speed and directions are shown on right. Panel B shows all composited soundings with the bolded dewpoint, temperature, and wind corresponding to the sounding observed on the date recording a DMO8 concentration in the middle of Moderate AQI categorical range (55 to 70 ppb) (27 July 2017; 63 ppb). Units for dewpoint and temperature are in °C, ms^{-1} for wind speed, and hectopascals (hPa) for pressure height.

The composited moderate (MD) versus exceedance (EXD) sounding reveals several noteworthy differences. First, EXD day mornings have slightly warmer PBL readings up to 1°C (Figs. 4.6a and 4.6b). Second, midlevel moisture is relatively higher considering dewpoint readings on the order of 4.5°C warmer between 500 hPa and 400 hPa (Figs. 4.6c and 4.6d).

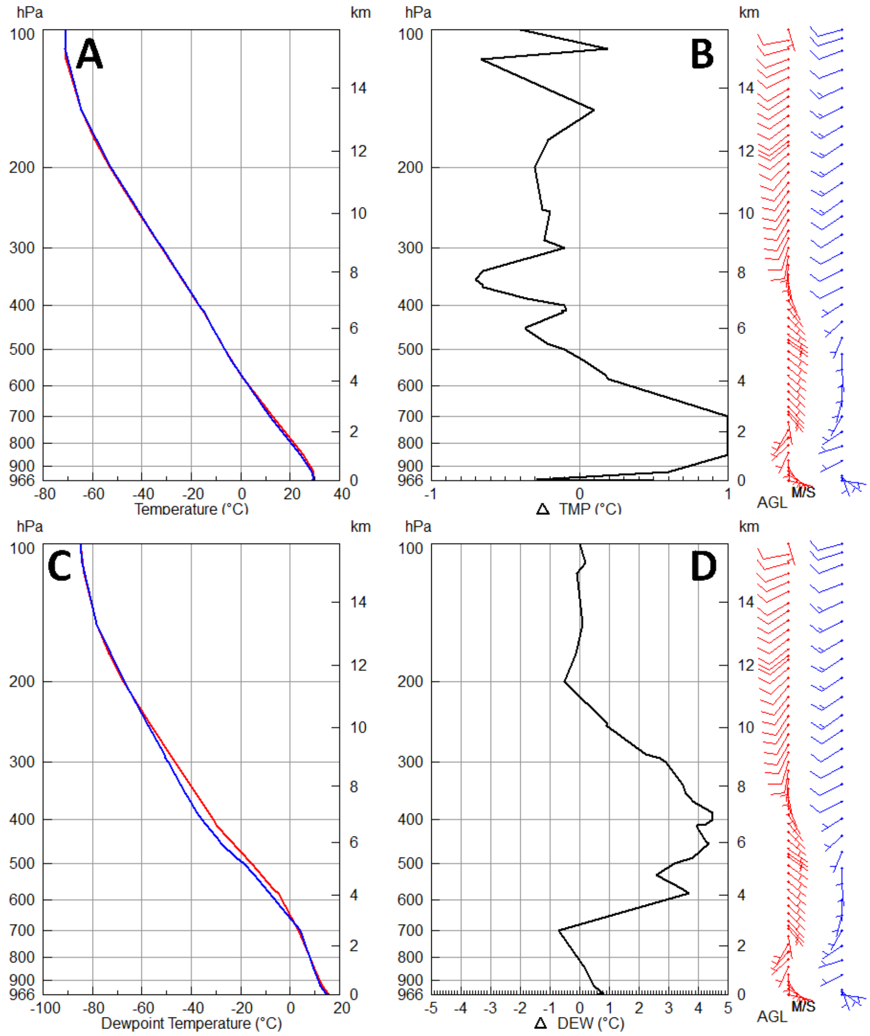

Fig. 4.6. Mean sounding profile comparison between Phoenix Nonattainment Area exceedance days (red) and Moderate Air Quality Index (AQI) days (blue) including temperature (A), temperature difference (B), dewpoint (C), and difference in dewpoint (D). Units for dewpoint and temperature are in °C, ms^{-1} for wind speed, and hectopascals (hPa) for pressure height.

Finally, dispersion patterns in terms of wind speed and direction are distinct. Specifically, weaker upper-level winds (Figs. 4.7a and 4.7b) and an easterly versus westerly wind component between the upper PBL (near 700 hPa) and 400 hPa pressure levels (Figs. 4.7c and 4.7d) favor EXD days. It is unclear at this time what is the direct influence of weaker upper-level winds on surface ozone concentrations; however, the identified easterly flow for higher ozone concentrations has been found to be significant for the Phoenix area (i.e., Malloy, 2018). This is due to the regional wind pattern flowing against the local mountain-valley circulation and likely contributing to an ozone rich layer over the city that fumigates toward the surface during periods of deep vertical mixing.

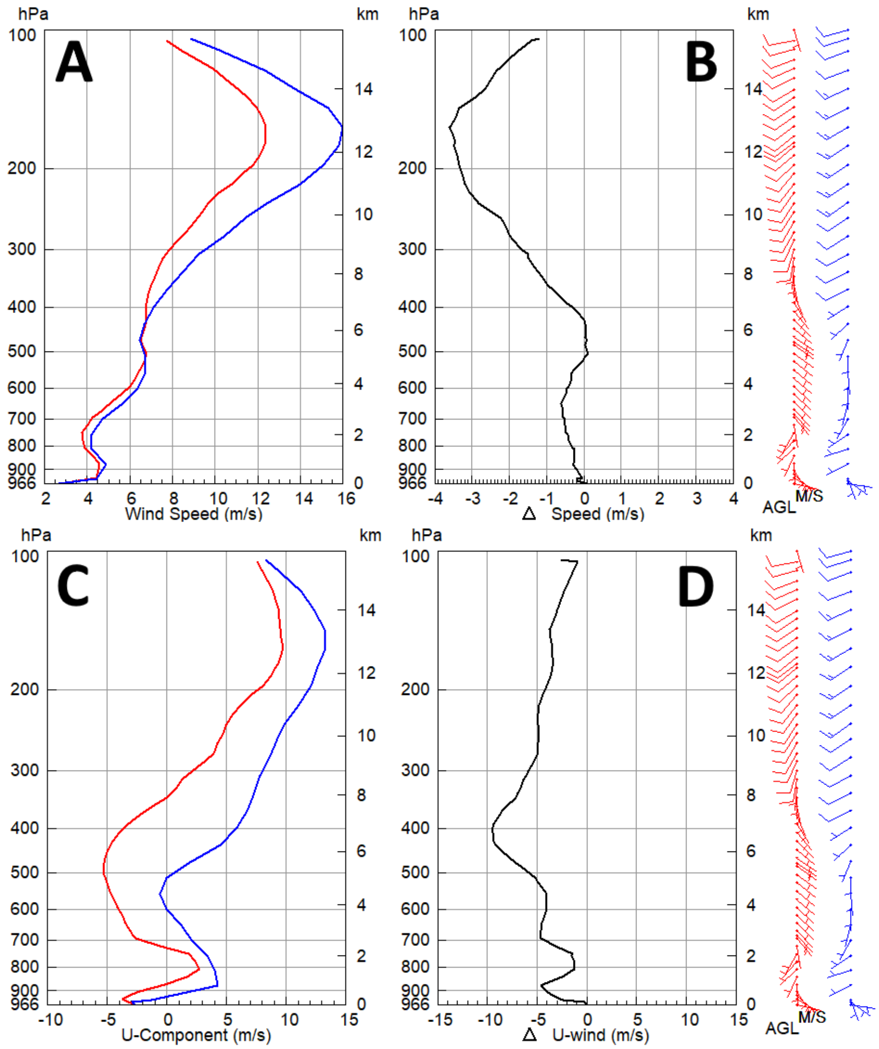

Fig. 4.7. Mean sounding profile comparison between Phoenix Nonattainment Area exceedance days (red) and Moderate Air Quality Index (AQI) days (blue) including wind speed (A), wind speed difference (B), zonal (U) wind component (C), and difference in zonal wind (D). Units for wind measurements are ms^{-1} and hectopascals (hPa) for pressure height.

Overall, early morning surface conditions are nearly identical when comparing MD and EXD days with temperatures around 29°C and wind speeds near 3 ms^{-1} displaying an easterly component. This reflects a documented persistent diurnal flow due to regional topography (Ellis et al., 1999). Major distinctions only arise higher in altitude demonstrating that a focus on surface considerations alone are not sufficient to forecast ozone levels.

Phoenix Ozone Good AQI Days

Unfortunately, for the Phoenix Nonattainment Area during the months of July and August, Good AQI ozone days (GD) are relatively rare with a sample size of only 84 out of 731 study days evaluated (11.4 percent). In relation to both EXD and MD days, large standard deviations for environmental dewpoint and wind speed at the midlevels and upper-levels, respectively, are also evident (Table 4.3).

Table 4.3
Phoenix, Arizona, 12Z composited sounding mean and standard deviations for temperature, dewpoint, and wind speed at significant pressure levels associated with ozone Good Air Quality Index days. Units for pressure are hectopascals (hPa), temperature and dewpoint are °C, and ms^{-1} for wind speed.

Pressure	Temperature		Dewpoint		Wind Speed	
	Mean	Std. Dev.	Mean	Std. Dev.	Mean	Std. Dev.
100	-70.4	2.4	-85.2	3.2	7.5	3.4
150	-64.8	2	-78.6	4.2	17.1	8.5
200	-52.4	1.4	-67.2	7	19.5	10.6
250	-41.2	1.6	-56.9	9.4	17.1	9.9
300	-31.9	2.1	-48.3	10.3	13.3	8.4
400	-16.6	1.8	-35.5	13.3	9.2	6.2
500	-6.3	1.6	-19.3	12.1	8.1	5.0
700	10.5	1.5	3.9	4.9	6.7	3.8
850	22.4	2.3	9.9	6	4.8	2.3
925	27.2	2.6	12.3	6.7	4.5	2.7
966(Surface)	27.8	2.2	15.1	5.4	2.9	2.7

The composited GD sounding is provided in Fig. 4.8a with the variability in individual profiles shown by Fig. 4.8b. The lowest observed DMO8 concentration over the study period was 38 ppb observed on 10 July 2015 and is highlighted in bold on Fig. 4.8b.

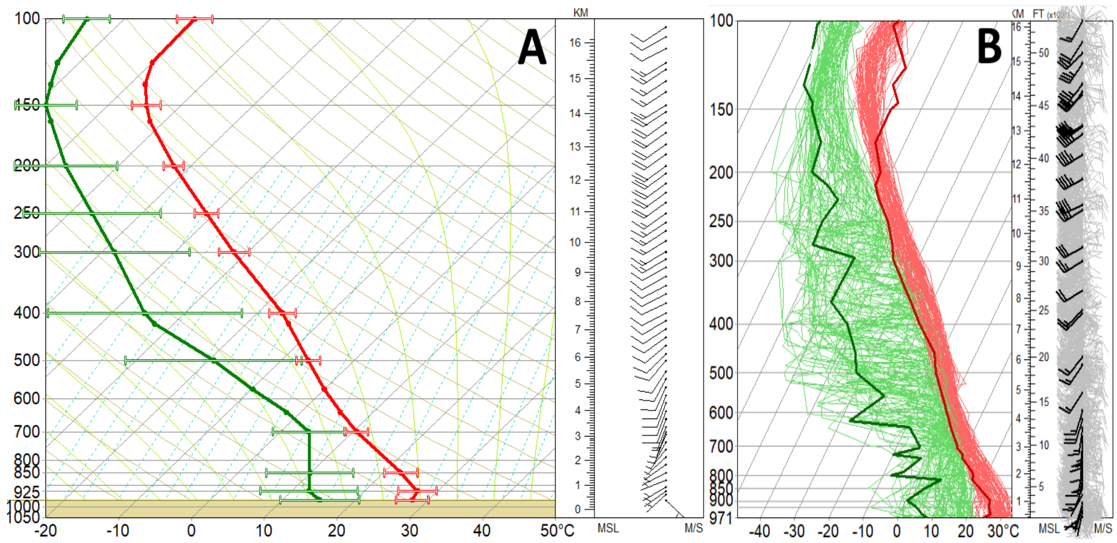

Fig. 4.8. Mean 12Z composite sounding for Phoenix ozone Good Air Quality Index (AQI) days (84) (A). Standard deviation bars at significant pressure levels are plotted for both the dewpoint (green) and temperature (red) mean profiles. Mean atmospheric wind speed and directions are shown on right. Panel B shows spaghetti plot of composited soundings with the bolded dewpoint, temperature, and wind corresponding to the sounding observed on the date with the lowest DMO8 concentration (10 July 2015; 38 parts per billion). Units for dewpoint and temperature are in °C, ms^{-1} for wind speed, and hectopascals (hPa) for pressure height.

When distinguishing between EXD days, GD are cooler in the PBL up to 3°C (Figs. 4.9a and 4.9b), and similar to the contrast between MD and EXD classifications, are drier in the midlevels with dewpoints around 4°C lower (Figs. 4.9c and 4.9d).

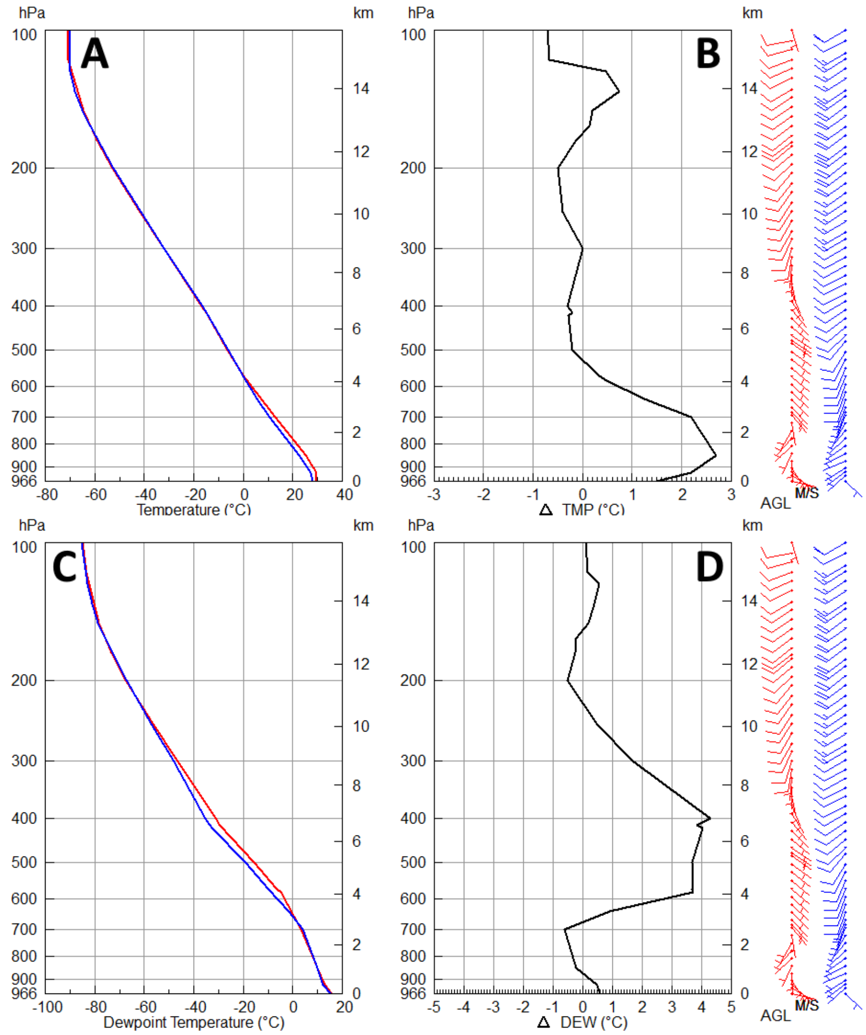

Fig. 4.9. Mean sounding profile comparison between Phoenix Nonattainment Area exceedance days (red) and Good Air Quality Index (AQI) days (blue) including temperature (A), temperature difference (B), dewpoint (C), and difference in dewpoint (D). Units for dewpoint and temperature are in °C, ms^{-1} for wind speed, and hectopascals (hPa) for pressure height.

The clear difference between GD and the EXD or MD groups is a deep and faster westerly flow (Fig. 4.10). Under this pattern, it is likely that 1) aged ozone aloft over the PNA would be transported downwind to limit local fumigation potential (e.g., Lee et al., 2003) and that 2) the diurnal ozone plume developing near the surface of the Phoenix urban area undergoes higher dispersion rates to reduce residency time over ozone monitoring sites. Consequently, DMO8 values are low.

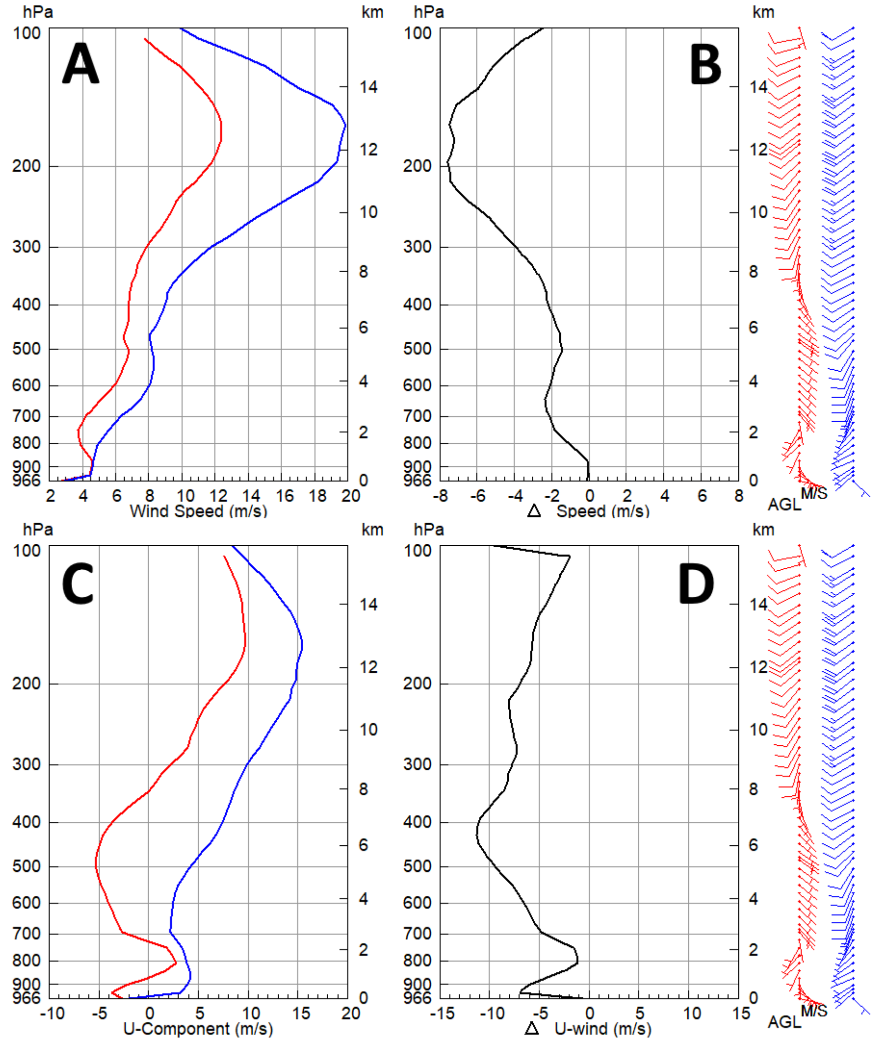

Fig. 4.10. Mean sounding profile comparison between Phoenix Nonattainment Area exceedance days (red) and Good Air Quality Index (AQI) days (blue) including wind speed (A), wind speed difference (B), zonal (U) wind component (C), and difference in zonal wind (D). Units for wind measurements are ms^{-1} and hectopascals (hPa) for pressure height.

Relationship with Synoptic Patterns

Two overriding characteristics are found to differentiate the EXD, MD, and GD type days. Specifically, midlevel moisture and 700-400 hPa wind direction. Influence on these parameters originates from overlying synoptic weather patterns. The regional placement of the NAM anticyclone circulation (namely at the 500 hPa level) plays a critical role for moisture transport creating “burst” and “break” periods in precipitation for the U.S. Southwest (Carleton, 1986). The NAM circulation’s relative core location to the PNA is also likely to influence dispersion patterns in the upper PBL. Therefore, 500 hPa height and 700 hPa vector winds daily composite plots were constructed for EXD (Figs. 4.11a and 4.11b), MD (Figs. 4.11c and 4.11d), and GD (Figs. 4.11e and 4.11f) groupings using the North American Regional Reanalysis dataset (NARR) (Mesinger et al., 2004).

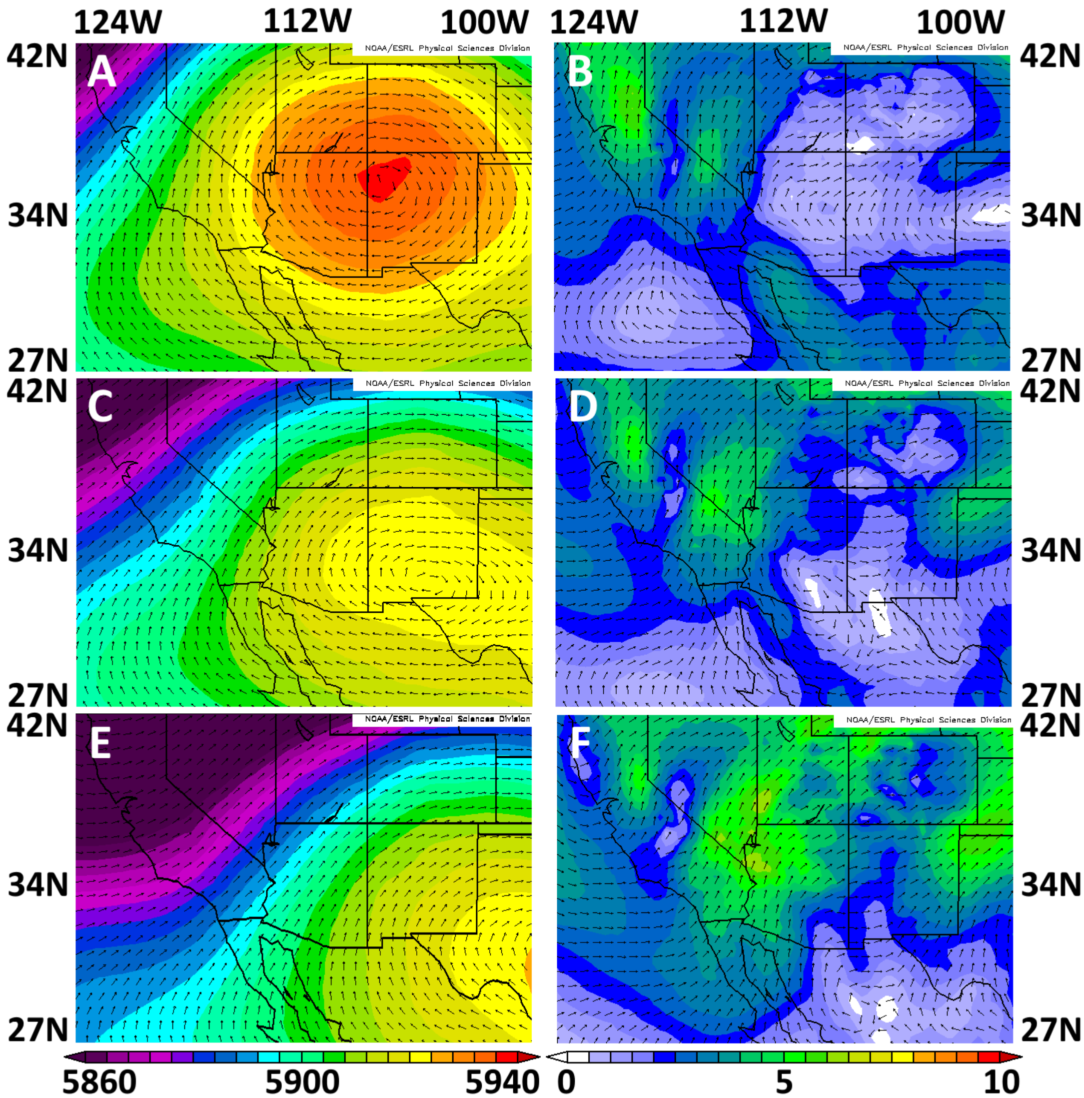

Fig. 4.11. Daily mean 500 hPa height and 700 vector wind speed plots for Phoenix ozone exceedance days (203) (A and B, respectively), Moderate Air Quality Index days (444) (C and D, respectively), and Good Air Quality Index days (84) (E and F, respectively). Units for height plots are in meters and ms^{-1} for vector wind speed. Images provided by the NOAA/ESRL Physical Science Division, Boulder, Colorado (2018).

Results reveal three synoptic types, including 1) a relatively strong anticyclone setup over the Colorado Plateau where UT, AZ, CO and NM border ("Four Corners," Fig. 4.11a) for EXD days, 2) weaker anticyclone circulation centered southeast of Phoenix near southern New Mexico for MD, and 3) Pacific troughing intruding the U.S.

Southwest suppressing the NAM circulation well to the south and east of Phoenix. Interestingly, the Four Corners High pattern is an ideal scenario to promote advection of moisture into Arizona, leading to convection and thunderstorms. This explains why the EXD composite sounding had higher dewpoints, at least in the midlevels of the atmosphere, compared to GD or MD days. Furthermore, this reinforces that a wind dispersion factor (speed and direction) versus moisture is likely more significant for ozone accumulation over the PNA.

The synoptic pattern over the U.S. Southwest is dynamic throughout the summer months (Adams and Comrie, 1997), so it should be expected that variations in temperature, moisture, and wind occurs as the NAM circulation “wobbles”. This would account for the large standard deviations in the atmosphere for each of the DMO8 categories, however, specific wind dispersion patterns seem to be necessary to allow ozone to either accumulate or disperse in the PNA. Based on the frequency and duration of EXD episodes (see Fig. 4.3) and GD events (Fig. 4.12), this study suggests there exists “pollution dispersion windows” that favor unhealthy or healthy air in Phoenix and likely the U.S. Southwest in general during the monsoon season. Evidence supports these pollution dispersion windows for good or bad air quality can be as short as a single day. Additionally, because moisture values, and therefore rainfall potential, were found to be erratic for the spectrum of DMO8 values analyzed in this study, it is likely that pollutant dispersion windows may not necessarily correspond with traditional monsoon precipitation burst and break periods.

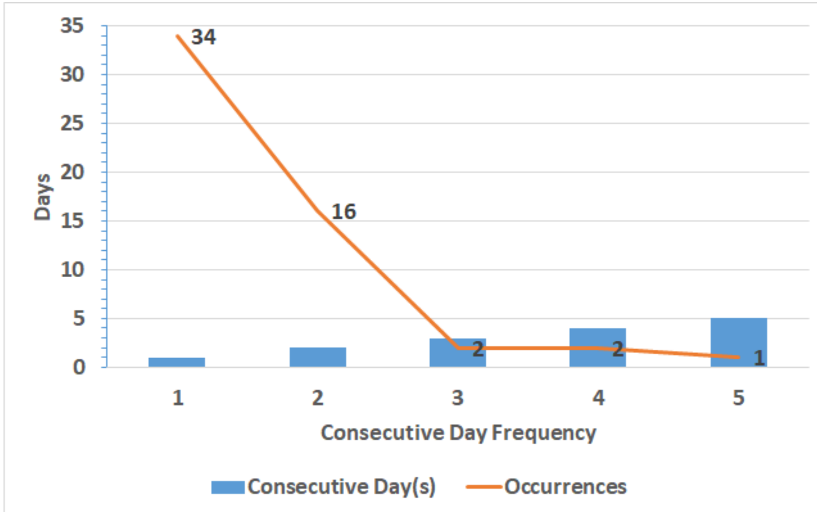

Fig. 4.12. Ozone Good Air Quality Index (AQI) day episode duration frequency for the Phoenix Nonattainment Area during the months of July and August (2006-2017).

Conclusions

Composite analysis of monsoonal July-August atmospheric soundings for the Phoenix Nonattainment Area (PNA) over the period 2006-2017 revealed that a large variability exists in vertical atmospheric conditions over the course of the North American Monsoon (NAM) and that higher surface ozone concentrations are possible for the PNA under numerous types of atmospheric combinations of moisture and temperature.

First, when reviewing soundings, wind characteristics appear to be a more reliable indicator than either moisture or temperature for an ideal atmosphere conducive for ozone accumulation. Specifically, light wind regimes with an easterly component between the upper PBL and midlevels of the atmosphere are prevalent based on the mean exceedance day composite sounding, while deep and faster westerly flow forces lower ozone concentrations.

Second, general synoptic patterns were found for Good, Moderate, and exceeding Air Quality Index (AQI) days. These patterns play a role for dictating large scale wind patterns and hence ozone accumulation potential for the Phoenix metropolitan.

Third, a “Four Corners High” position (central Colorado Plateau) of the monsoon midlevel circulation was identified as a favorable synoptic setup for higher DMO8 values, despite a flow pattern that would be conducive for moisture transport into the PNA. On the other hand, closer proximity to Pacific troughing enhances dispersion of ozone at both the surface and aloft. Consequently, analogous to precipitation “bursts” and “breaks” this study has determined “pollution dispersion windows” that provide a conceptual model framework for general air quality expectations.

Fourth, throughout the study period, single day ozone exceedance occurs at a much higher frequency versus longer durations, suggesting that even short day-to-day migration of the monsoon circulation are important for pollutant potential in this region. Additionally, using the U.S. EPA’s current threshold for healthy air (DMO8 $\leq$55 ppb), the months of July and August rarely see atmospheric conditions supportive of high dispersion rates (i.e., deep westerly flow) sufficient enough declare a Good AQI day.

Finally, although a light easterly synoptic flow relative to Phoenix’s unique topography is significant for locally unhealthful ozone levels, it is suspected, but not confirmed in this study, that a deep westerly flow pattern associated with Pacific troughing causes a regional decrease in ozone levels for urbanized areas due to higher dispersion rates. However, background ozone concentrations downwind of these urban sites may increase due to transport mixing mechanisms.

Findings presented in this study demonstrate composite sounding analysis is a viable and useful forecasting technique for air quality applications. Results are expected to be particularly pertinent to air quality meteorologists responsible for disseminating ozone forecasts within and in proximity to the Phoenix Nonattainment Area.

CHAPTER 5

CONCLUSIONS

Summary of Research Intent

The threats from summer monsoon related hazards represent a common and recurring concern for residents in the American Southwest once the North American Monsoon (NAM) becomes established over the region. Unfortunately, protection of life and property from blinding blowing dust, deadly lightning, sudden flash floods, damaging thunderstorm winds, severe hail, heat related illness, suspended dust inhalation, and unhealthy ozone exposure become compromised due to inadequate lead warning time for risk recognition. This issue is rooted in forecast uncertainty concerning what are the ideal conditions promoting threat development. In brief, predicting direct and indirect monsoon hazards (e.g., severe hail versus ozone dispersion) is problematic. Ultimately, the large-scale weather pattern controlling intra-seasonal moisture advection, atmospheric instability, and wind regimes during the NAM is far from static. Rather, environmental conditions through the atmospheric column can be highly variable, evolving in space and time, between the onset and demise of the monsoon circulation. Notably, this means forecast accuracy would suffer attempting to determine the likelihood specific hazards could develop at particular locations without first considering the dynamic nature of the vertical atmosphere.

Overcoming the challenging aspect of an evolving monsoon circulation can be addressed by linking a monsoon hazard with the vertical state of the atmosphere. Therefore, the focus of this dissertation has been using upper-air sounding data to document recurring atmospheric types for hazard identification. I have completed three studies that each addresses a part of my following research question: What is the viability for limited available in-situ sounding data in the American Southwest to identify ideal atmospheric conditions for independent monsoon hazards? Explicitly, I investigated the following:

1) Identifying upper-air characteristics of severe hail versus non-severe hail days over the Arizona portion of the Colorado Plateau,

2) determining whether upper-air measurements are statistically significant between unhealthy and healthy ozone concentrations observed in the Phoenix metropolitan, and

3) finding specific vertical profiles of temperature, moisture, and wind influencing ozone accumulation potential in Phoenix.

The overarching research question has led to my fundamental research hypothesis: There are repeating atmospheric alignments, measured by in-situ sounding data, concerning geopotential height, air temperature, dew point, dew point depression, and wind occurring during the NAM that are conducive to specific and independent monsoon hazards (e.g., severe hail over the Colorado Plateau and exceeding ozone levels in Phoenix, Arizona). As a result, the use of sounding data will be found to be applicable discerning favorable time periods when atmospheric conditions warrant the imminence of particular hazards as the monsoon circulation continues shifting position and intensity throughout a season.

Summary of Results

My first study utilized 12Z (0500 LST) Flagstaff sounding data for the Colorado Plateau area of northern Arizona to explore severe hail potential. A total of 30 sounding parameters for severe hail days from 1996 to 2009 were found to be statistically significant at certain thresholds to the 0.05 significance level (i.e., p-value ≤ 0.05) using the Smith-Welch-Satterwaite test. However, their presence was also evident on non-severe hail days at times. Potential reasons are two-fold. First, study days (severe versus non-severe hail) were stratified based on the National Climatic Data Center's Storm Events Database that relies on severe weather reports from National Weather Service Storm Spotters, public safety officers, media, and general public. Due to remoteness of the Arizona portion of the Colorado Plateau study area, a subset of non-severe hail days was likely misclassified as severe hail occurrences went undocumented. Secondly, the discrepancy may reflect the evolution of the monsoon circulation, where there is a lag in changes between low, middle, and upper atmospheric parameters. In essence, this reveals that the severe hail hazard over the Colorado Plateau (and likely throughout the U.S. Southwest) is possible under multiple atmospheric configurations of temperature, moisture, and wind profiles. This highlights the complexity for predicting this particular monsoon hazard. Even so, general conclusions are possible about a favorable environment by reviewing the relative frequency of statistically significant parameters present on severe hail sounding profiles and their absence on non-severe hail days. Results indicate severe hail episodes in northern Arizona favor a relative warm, moist, and predominately deep light south to southeasterly flow throughout the atmospheric column, except for a southwesterly 700 hPa wind direction. This is in contrast to deep and drier southwesterly flow typical on non-severe hail days.

My second study addressed the indirect monsoon hazard of excessive ozone accumulation for the Phoenix metropolitan. Phoenix sounding data between 2006 and 2016 were first analyzed using the nonparametric Monte Carlo Permutation two-sample test comparing days when the daily maximum 8-hour ozone average (DMO8) exceeded the U.S. EPA standard against those days that were observed below the 70 parts per billion (ppb) standard. Both 12Z and 00Z (0500 and 1700 LST) rawinsondes were reviewed for significant parameters. A total of 23 and 17 parameters for 0500 and 1700 LST, respectively, demonstrated significance to the 0.01 level (i.e., p-value ≤ 0.01). Importantly, parameters in the middle and upper atmosphere, in addition to PBL parameters, were discovered, showing a link between the large-scale monsoon circulation and ground-level ozone concentrations. After statistical significance for several sounding variables were established, I then used principal component analysis (PCA) and linear discriminant analysis with a cross validation check to create synoptic composite maps for accurately and inaccurately predicted ozone exceedance and non-exceedance days. Results revealed primary synoptic patterns with unique differences in temperature, moisture, and wind characteristics favoring either unhealthy and healthy days.

Specifically, a monsoon circulation positioned near the Four Corners vicinity (central Colorado Plateau) induces light easterly flow over the Phoenix metropolitan area between 700 and 400 hPa pressure levels that has been found to be prevalent on days with unhealthy ozone concentrations for the city. An easterly flow near the 700 hPa pressure level corresponds to the typical summertime upper planetary boundary layer

(PBL) and would counter a previously documented local daytime mountain-valley circulation. It is suspected, but not confirmed in my research, this is a mechanism leading to ozone accumulation aloft made available for fumigation by convective down-mixing processes during the daytime expansion of the PBL to increase ozone concentrations near the surface.

For healthy ozone days, a suppressed monsoon circulation in strength and latitude caused by low-pressure troughing over the U.S. West Coast promotes deeper and relatively faster westerly flow over the city of Phoenix to enhance pollutant dispersion throughout the PBL leading to a corresponding drop in ozone accumulation potential. Westerly winds would also align with the local daytime diurnal mountain-valley circulation pattern to facilitate pollutant dispersion downwind of Phoenix. It is reasoned, but not validated in my research, that a deep westerly flow pattern associated with Pacific troughing causes a regional decrease in ozone levels for urbanized areas due to higher dispersion rates. However, background ozone concentrations downwind of these urban sites may increase due to transport mixing mechanisms.

Additionally, a secondary synoptic setup favoring non-exceeding ozone values was found which resembles a previously identified active thunderstorm pattern for central Arizona. In this case a monsoon circulation situated east of Arizona forces moist southeasterly flow into the region to fuel widespread thunderstorm development by steering convection off higher terrain features into the lower deserts.

A final noteworthy result of the second study is that the ozone precursor variables of oxides of nitrogen and carbon monoxide (24-hour mean values) observed in the urban core region of the Phoenix metropolitan were found to not be statistically significant to the *p*-value ≤0.01 for distinguishing exceeding versus non-exceeding DMO8 days. It is reasoned that this finding supports that meteorological dispersion patterns for the months of July and August have a greater influence on local ozone concentration potential versus any day-to-day variability for anthropogenic emission releases (e.g., the “weekend effect”).

My third study differed from the second research paper with a more detailed assessment investigating the interplay of temperature, moisture, and wind measured on Phoenix vertical atmospheric profiles relative to high and low ozone concentration days. The study period is between 2006 and 2017 and emphasizes the morning (i.e., 0500 LST) rawinsonde launches to understand the environment favorable for daily ozone accumulation leading to maximum DMO8 concentrations that typically peak in the late afternoon hours for the Phoenix study area. DMO8 values were separated into three groupings based on the U.S. EPA’s Air Quality Index (AQI) categories constrained to the following unique ppb ranges representing specific health impacts, 1) “Good” (0-54 ppb), “Moderate” (55-69 ppb), and collectively the AQI categories exceeding the U.S. EPA health standard of 70 ppb. Composite atmospheric sounding analysis was used to determine common distinctions and variability for temperature, moisture, and wind between DMO8 classifications.

Composite sounding analysis for Good, Moderate, and exceeding ozone AQI days reveal that both temperature and moisture are not reliable indicators for anticipating ozone concentration potential over the Phoenix metropolitan area. Small standard deviations in temperature were found throughout the atmospheric column, while large standard deviations in dewpoint over 10°C were identified in the mid-levels of the atmosphere (500-400 hPa) for all three AQI tiers ranging from healthy to unhealthy ozone. Rather, it was discovered that wind speed and orientation are better indicators versus temperature and moisture for forecasting ozone concentration range. Specifically, exceedance days reveal an apparent unique easterly component flow regime between 700 and 400 hPa and lighter winds in general in the vertical. Contrastingly, Good AQI days tend to have deep and faster westerly flow. The typical Moderate AQI day wind profile, having largely light but southerly to southwesterly winds, is believed to represent the transition period between atmospheric vertical states conducive for the two pollutant concentration extremes.

Furthermore, results show that Good AQI ozone days for the Phoenix metropolitan should be considered rare for the months of July and August compared to Moderate AQI or exceeding days by being observed only 11.4 percent of the study period. Additionally, Good AQI events tend to last no more than one to two days at a time, but have reached up to five consecutive days. Exceeding days occur at a greater frequency during the monsoon season (27.7 percent of the study period), however, similar to Good AQI events the majority of unhealthy air quality episodes are restricted at one to two-day intervals, but have spanned a maximum of 13 consecutive days. Therefore, pollutant dispersion windows, or in other words, conditions associated with ideal ozone accumulation or dispersal (i.e., exceeding or Good AQI days) tend to be short-lived lasting less than two days at a time. These findings highlight that even small strength and positioning changes of the monsoon circulation affecting wind flow may be significant for air quality forecasting purposes.

Finally, because 1) moisture has been found to be highly variable across a spectrum of observed DMO8 values and 2) air quality episodes, whether healthy or unhealthy, are usually short in duration, the discovered pollutant dispersion windows are not expected to correspond to the traditional monsoon “burst” and “break” precipitation periods that have been found to typically last several days at a time.

Overall Conclusions

The three studies assessing the usefulness of upper-air data toward monsoon hazard forecasting produced mixed results concerning my hypotheses. Although it is confirmed that monsoon hazard prediction for both severe hail on the Colorado Plateau and unhealthy ozone events in Phoenix can be aided by using in-situ upper-air sounding data, it has also been determined that these independent hazards can occur under a spectrum of ideal atmospheric states. Broadly expressed, I hypothesized that, as a variable monsoon circulation “wobbles” both in strength and position over the U.S. Southwest, there will exist recurring and distinct patterns in the vertical structure of the atmosphere relative to the Colorado Plateau and the Phoenix metropolitan area that favor severe hail development and elevated ground-level ozone concentrations. A major conclusion, however, is that specific hazard development occurs when atmospheric parameters reaching identified significant threshold ranges begin to overlap, generating myriad possible vertical configurations in temperature, moisture, and wind conducive for hazard formation. In other words, prediction of severe hail and excessive ozone accumulation (and likely other monsoon hazards) are dependent upon the intra-seasonal migration of the monsoon circulation and subsequent lag in changing vertical atmospheric conditions. Therefore, monsoon hazard forecasting should not rely on a single significant parameter or a discrete atmospheric profile as hypothesized would exist. It is generally concluded that forecasting needs to take into account a range of possible atmospheres. This finding invalidated limited parts of my initial hypotheses.

Specific to severe hail, I had hypothesized that occurrences of this hazard on the Colorado Plateau will demonstrate a vertical profile indicative of a monsoon circulation placement offset toward the east of the Colorado Plateau that draws low-level moisture into the region from the south and southeast around the periphery of the anticyclone. The offset location also prevents strong subsidence aloft inherent with the upper-atmospheric anticyclone center that typically suppresses thunderstorm development. Additionally, the eastward shift in the anticyclone would allow possible intrusion of cooler air aloft from Pacific troughing over the western U.S. to aid in destabilizing the atmosphere for thunderstorms to reach severe limits. As a result, there would be an ideal profile revealing warm, moist low and mid-levels with southeasterly advection occurring beneath a drier, cooler upper atmosphere with southwesterly flow; a combination that represents an unstable convective vertical profile.

Although I was unable to find an explicit sounding profile type encouraging severe hail as hypothesized, I have confirmed that the position of the mid-level monsoon circulation influencing regional temperature, moisture, and wind patterns, and hence the vertical profile shown by in-situ sounding data, is significant for predicting severe hail development over northern Arizona.

Concerning ozone concentrations in Phoenix, I first hypothesized that there would exist an array of sounding parameters above the surface that show statistically significant differences in association with unhealthy and healthy ozone days. Specifically, variables included temperature, moisture, wind speed. Ultimately, vertical atmospheric traces suitable for enhanced ozone accumulation in the PNA would depict a monsoon circulation nearly centered overhead. Placement would create 1) a weak pressure gradient to lower wind speeds and pollutant dispersion throughout column and 2) limit thunderstorm activity and cloud cover to interfere with sunlight necessary for new ozone formation. Therefore, periods of high ozone would follow "burst" and "break" periods in rainfall. Furthermore, concerning ozone dispersion, wind speed versus prevailing wind direction, especially in the planetary boundary layer, is reasoned to play a larger role. This conjecture is based on prior studies indicating a persistent mountain-valley circulation in the Phoenix area during the monsoon period (Ellis et al., 1999).

These hypotheses were only partially confirmed. My second research paper proved that temperature, moisture, and wind elements were statistically significant above the surface distinguishing healthy versus unhealthy ozone days, however, a primary ozone exceedance pattern for Phoenix was a "Four Corners High" position with light easterly flow in the upper PBL over the metropolitan. This means that both wind speed and wind direction need to be considered for air quality forecasting purposes. The finding of upper PBL wind direction countering the typical mountain-valley circulation being significant also points to the necessity that mechanisms for ozone accumulation and transport are more complex than reviewing near-surface dispersion characteristics alone. Finally, my third research paper found periods of exceeding ozone and healthy ozone concentration days likely do not follow the well-established monsoon precipitation "burst" and "break" cycle due to a majority of episode event durations lasting two days or less. This is an important finding because it indicates that there likely exist other unique monsoon hazard cycles sensitive to changing atmospheric pattern alignments.

Following confirmation that significant sounding parameters exist to differentiate days when ozone will exceed the U.S. EPA standard, I next hypothesized that by using atmospheric composite sounding analysis, I can identify common vertical profiles that exist for varying ranges of observed ozone concentrations in Phoenix.

Results from my third research paper did indicate a suite of vertical profiles that are supportive of healthy and unhealthy ozone. Discrepancies in wind speed and direction, however, between ozone AQI categories were pronounced versus either temperature or moisture. Generally, vertical temperature had little variability amongst the different ozone ranges. Vertical moisture did exhibit a large deviance for all ozone concentration groupings, including near saturation in the mid-levels of the atmosphere noted on some vertical profiles. This suggests there is an ozone accumulation persistence factor given that high levels of ozone have been observed during times with abundant moisture and cloud cover that would normally interfere with the photochemistry to form new ozone.

Fundamentally, I hypothesized that statistical significance for geopotential height, air temperature, dew point, dew point depression, wind speed, and wind direction parameters extending throughout the atmospheric column, as measured by soundings, will be found in association with severe hail and ozone accumulation environment identification. Therefore, sounding data will be viable tools to forecast these hazards by finding ideal atmospheric combinations highlighting risk potential. Ultimately, all of the results from my three studies support this fundamental hypothesis.

Significance

Monsoon hazards adversely affect our community, economy, and environment. The body of research for the North American Monsoon continues to mature, however, understanding of the principles favoring hazard development, although progressing, is incomplete; a reality that challenges today's meteorologists responsible for warning a vulnerable public existing throughout the American Southwest. To aid creating a robust knowledge regarding a complex monsoon phenomenon, this dissertation assessed the application of using limited regional in-situ upper-air sounding data to address two common but independent monsoon hazards. Namely, severe hail over the Colorado Plateau and unhealthful ozone in the Phoenix metropolitan. I have statistically confirmed the significance of the vertical atmosphere and importance of an evolving monsoon circulation with respect to the onset for both investigated hazards.

Fundamentally, my research has demonstrated that monsoon studies require review of a dynamic monsoon atmosphere extending beyond the surface or near-surface. My work provides a repeatable research framework laying the foundation for future efforts linking the vertical atmosphere to other monsoon hazards since confident and accurate hazard prediction are essential to protect our infrastructure and save future lives.

REFERENCES

Arizona Department of Environmental Quality (ADEQ) High Pollution Advisories, 2019. http://www.azdeq.gov/programs/air-quality-programs/air-forecasting. November 1, 2019.

Adams, D. K. and A. C. Comrie, 1997. The North American monsoon. *Bulletin of the American Meteorological Society*, **78**, 2197-2213.

Adang, T. C. and R. L. Gall, 1989. Structure and dynamics of the Arizona monsoon Boundary. *Monthly Weather Review*, **117**, 1423-1438.

Alghamdi, M. A., M. Khoder, R. M. Harrison, A. P. Hyvarinen, T. Hussein, H. Al-Jeelani, A. S. Abdelmaksoud, M. H. Goknil, I. I. Shabbaj, F. M. Almehmadi, H. Lihavainen, M. Kulmala, and K. Hameri, 2014. Temporal variations of O_3 and NO_x in the urban background atmosphere of the coastal city Jeddah, Saudi Arabia. *Atmospheric Environment*, **94**, 205-214.

Atkinson-Palombo, C. M., J. A. Miller, and R. C. Balling, 2006. Quantifying the ozone "weekend effect" at various locations in Phoenix, Arizona. *Atmospheric Environment*, **40**, 7644-7658.

Balling, R. C. and S. W. Brazel, 1987. Diurnal-variations in Arizona monsoon precipitation frequencies. *Monthly Weather Review*, **115(1)**, 342-346.

Brazel, A. J. and W. G. Nickling, 1986. The relationship of weather types to duststorm generation in Arizona (1965-1980). *Journal of Climatology*, **6**, 255-275.

Bhushan, S. and A. P. Barros, 2007. A numerical study to investigate the relationship between moisture convergence patterns and orography in central Mexico. *Journal of Hydrometeorology*, **8(6)**, 1264-1284.

Bunkers, M. J., J. R. Wetenkamp, Jr., and J. J. Schild, 2010. Observations of the relationship between 700-mb temperatures and severe weather reports across the contiguous United States. *Weather and Forecasting*, **25**, 799-814.

Burt, J. E. and G. M. Barber, 1996. Elementary Statistics for Geographers. *The Guilford Press*, New York, New York.

Carleton, A. M., 1986. Synoptic-dynamic character of “bursts” and “breaks” in the southwest
U.S. summer precipitation singularity. *Journal of Climatology*, **6**, 605-623.

Davis, J.C., 1986. Statistics and Data Analysis in Geology. John Wiley & Sons.

Desilets, S. L. E., T. P. A. Ferre, and B. Ekwurzel, 2008. Flash flood dynamics and composition in a semiarid mountain watershed. *Water Resources Research*, **44**, 1-13.

Diem, J. and D. Brown, 2009. Relationships among monsoon-season circulation patterns, gulf surges, and rainfall within the Lower Colorado River Basin, USA. *Theoretical and Applied Climatology*, **97(3-4)**, 373-383.

Douglas, M. W., R. A. Maddox, K. Howard, and S. Reyes, 1993. The Mexican Monsoon. *Journal of Climate*, **6(8)**, 1665-1677.

Dunea, D., S. Lordache, D. C. Alexandrescu, and N. Dinca, 2014. Screening the weekdays/weekend patterns of air pollutant concentrations recorded in southeastern Romania. *Environmental Engineering and Management Journal*, **13**, 3105-3114.

Ellis, A. W., M. L. Hildebrandt, and H. J. S. Fernando, 1999. Evidence of lower-atmospheric ozone "sloshing" in an urbanized valley. *Physical Geography*, **20**, 520-536.

Ellis, A. W., M. L. Hildebrandt, W. H. Thomas, and H. J. S. Fernando, 2000. Analysis of the climatic mechanisms contributing to the summertime transport of lower atmospheric ozone across metropolitan Phoenix, Arizona, USA. *Climate Research*, **15,** 13-31.

Ellis, A. W., E. M. Saffell, and T. W. Hawkins, 2004. Method for defining monsoon onset and demise in the Southwestern USA. *International Journal of Climatology*, **24**, 247-265.

Evans, C., S. J. Weiss, I. L. Jirak, A. R. Dean, and D. S. Nevius, 2018. An evaluation of Paired regional/convection-allowing forecast vertical thermodynamic profiles in warm-season, thunderstorm-supporting environments. *Weather and Forecasting*, **33**, 1547-1566.

Fast, J. D., J. C. Doran, W. J. Shaw, R. L. Coulter, and T. J. Martin, 2000. The evolution of the boundary layer and its effect on air chemistry in the Phoenix area. *Journal of Geophysical Research-Atmospheres*, **105**, 22833-22848.

Fawbush, M., Miller, R., and Starrett, L., 1951. An Empirical Method of Forecasting Tornado Development. *Bulletin of the American Meteorological Society*, **32(1)**, 1-9.

Filliben, J. J., 1975. The Probability Plot Correlation Coefficient test for normality. *Technometrics*, **17(1)**, 111-117.

Gaffen, D., 1996. A digitized metadata set of global upper-air station histories. NOAA Technical Memorandum ERL ARL-211. *National Oceanic and Atmospheric Administration*, 1-43.

Giaiotti, D. B. and F. Stel, 2007. A multiscale observational case study of an isolated tornadic supercell. *Atmospheric Research*, **83**, 152-161.

Gold, D. R., G. Allen, A. Damokosh, P. Serrano, C. Hayes, and M. Castillejos, 1996. Comparison of outdoor and classroom ozone exposures for school children in Mexico City. *Journal of the Air & Waste Management Association*, **46**, 335-342.

Goudie, A. S., 2014. Desert dust and human health disorders. *Environmental International*, **63**, 101-113.

Harlan, S. L., A. J. Brazel, L. Prashad, W. L. Stefanov, and L. Larsen, 2006. Neighborhood microclimates and vulnerability to heat stress. *Social Science & Medicine*, **63**, 2847-2863.

Heinselman, P. L., and D. M. Schultz, 2006. Intraseasonal variability of summer storms over central Arizona during 1997 and 1999. *Weather and Forecasting*, **21**, 559-578.

Higgins, R. W., W. Shi, and C. Hain, 2004. Relationships between Gulf of California moisture surges and precipitation in the southwestern United States. *Journal of Climate,* **17(15)**, 2983-2997.

Higgins, R. W. and W. Shi., 2005. Relationships between Gulf of California moisture surges and tropical cyclones in the eastern Pacific basin. *Journal of Climate*, **18(22)**, 4601-4620.

Johnson, R. H., P. E. Ciesielski, B. D. McNoldy, P. J. Rogers, and R. K. Taft, 2007. Multiscale variability of the flow during the North American Monsoon Experiment. *Journal of Climate*, **20(9)**, 1628-1648.

King, T. S., and R. C. Balling, 1994. Diurnal-variations in Arizona monsoon lightning data. *Monthly Weather Review*, **122(7)**, 1659-1664.

King, A. T. and A. D. Kennedy, 2019. North American supercell environments in atmospheric reanalyses and RUC-2. *Journal of Applied Meteorology and Climatology*, **58(1)**, 71-92.

Kirshbaum, D. J. and D. R. Durran, 2004. Factors governing cellular convection in orographic precipitation. *Journal of the Atmospheric Sciences*, **61(6)**, 682-698.

Lee, S. M. and H. J. S. Fernando, 2013. Dispersion of an urban photochemical plume in Phoenix metropolitan area. *Atmospheric Environment*, **80**, 152-160.

Lee, S. M., H. J. S. Fernando, M. Princevac, D. Zajic, M. Sinesi, J. L. McCulley, and J. Anderson, 2003. Transport and diffusion of ozone in the nocturnal and morning planetary boundary layer of the Phoenix valley. *Environmental Fluid Mechanics*, **3**, 331-362.

Maddox, R. A., D. M. McCollum, and K. W. Howard, 1995. Large-scale patterns associated with severe summertime thunderstorms over central Arizona. *Weather and Forecasting*, **10(4)**, 763-778.

Malloy, J. W., 2011. Using atmospheric profiles to forecast severe hail events in northern Arizona during the North American Monsoon season. *Journal of the Arizona-Nevada Academy of Science*, **43(1)**, 16-26.

Malloy, J. W., 2018. Atmospheric patterns in relationship with observed ozone concentrations in the Phoenix, Arizona, metropolitan area during the North American Monsoon. *Atmospheric Environment*, **191**, 64-69.

McCollum, D. M., R. A. Maddox, and K. W. Howard, 1995. Case-study of a severe mesoscale convective system in central Arizona. *Weather and Forecasting*, **10(3)**, 643-665.

Mesinger, F., DiMego, G., Kalnay, E., Mitchell, K., Shafran, P. C., Ebisuzaki, W., Jovic, D., Woollen, J., Rogers, E., Berbery, E. H., Ek, M. B., Fan, Y., Grumbine, R., Higgins, W., Li, H., Lin, Y., Manikin, G., Parrish, D. and W. Shi, 2004. North American regional reanalysis: A long-term, consistent, high-resolution climate dataset for the North American domain, as a major improvement upon the earlier global reanalysis datasets in both resolution and accuracy. *Bulletin of the American Meteorological Society*, **87**, 343-360.

Michaud, J. D., B. A. Auvine, and O. C. Penalba, 1995. Spatial and elevational variations of summer rainfall in the Southwestern United-States. *Journal of Applied Meteorology*, **34(12)**, 2689-2703.

Middleton, N. J., 2017. Desert dust hazards: A global review. *Aeolian Research*, **24**, 53-63.

Mills, G., Harmens, H., Wagg, S., Sharps, K., Hayes, F., Fowler, D., Sutton, D., Sutton, M. and B. Davies, 2016. Ozone impacts on vegetation in a nitrogen enriched and changing climate. *Environmental Pollution*, **208**, 898-908.

Mitchell, D. L., D. Ivanova, R. Rabin, T. J. Brown, and K. Redmond, 2002. Gulf of California sea surface temperatures and the North American monsoon: Mechanistic implications from observations. *Journal of Climate*, **15(17)**, 2261-2281.

Monks, P. S., A. T. Archibald, A. Colette, O. Cooper, M. Coyles, R. Derwent, D. Fowler, C. Granier, K. S. Laws, G. E. Mills, D. S. Stevenson, O. Tarasova, V. Thouret, E. von Schneidemesser, and R. Sommariva, 2015. Tropospheric ozone and its precursors from the urban to the global scale from air quality to short-lived climate forcer. *Atmospheric Chemistry and Physics*, **15**, 8889-8973.

Moore, T. J., R. L. Gall, and T. C. Adang, 1989. Disturbances along the Arizona monsoon boundary. *Monthly Weather Review*, **117(5)**, 932-941.

Mullen, S. L., J. T. Schmitz, and T. C. Adang, 1998. Intraseasonal variability of the summer monsoon over southeast Arizona. *Monthly Weather Review*, **126(11)**, 3016-3035.

National Climatic Data Center (NCDC), 2010. National Climatic Data Center Storm Events Database. *National Climatic Data Center*.

National Oceanic Atmospheric Administration/Earth Systems Research Laboratory Physical Science Division, Boulder, Colorado, 2018. http://www.esrl.noaa.gov/psd. May 30, 2018.

National Oceanic Atmospheric Administration/Earth Systems Research Laboratory Physical Science Division, Boulder, Colorado, 2018. http://www.esrl.noaa.gov/psd. October 4, 2018.

Owens, E. O., Patel, M. M., Kirrane, E., Long, T. C., Brown, J., Cote, I., Ross, M. A. and S. J. Dutton, 2017. Framework for assessing causality of air pollution-related health effects for reviews of the National Ambient Air Quality Standards. *Regulatory Toxicology and Pharmacology*, **88**, 332-337.

Quincy, P., Butterfield, D., D'Souza, H. and M. Henderson, 2007. Monitoring of ozone precursors in ambient air using pumped and diffusive sampling on the sorbent Carbopack X. *Atmospheric Environment*, **41**, 7865-7873.

Ramage, C. S., 1971. Monsoon meteorology. *International Geophysics Series*, **15**, 296.

Raman, A., A. F. Arellano Jr., and J. J. Brost, 2014. Revisiting haboobs in the southwestern United States: An observational case study of the 5 July 2011 Phoenix dust storm. *Atmospheric Environment*, **89**, 179-188.

RAOB, 2018. The Universal RAwindsonde Observation Program. https://www.raob.com.

Rasmussen, D. J., A. M. Fiore, V. Naik, L. W. Horowitz, S. J. McGinnis, and M. G. Schultz, 2012. Surface ozone-temperature relationships in the eastern US: A monthly climatology for evaluating chemistry-climate models. *Atmospheric Environment*, **47**, 142-153.

Rodriquez, C. A. M., R. P. da Rocha, and R. Bombardi, 2010. On the development of summer thunderstorms in the city of Sao Paulo: Mean meteorological characteristics and pollution effect. *Atmospheric Research*, **96**, 477-488.

Rodriquez, O. and J. Bech, 2014. Souding-derived parameters associated with tornadic storms in Catalonia. *International Journal of Climatology*, **38**, 2400-2414.

Rowe, A. K., S. A. Rutledge, T. J. Lang, P. E. Ciesielski, and S. M. Saleeby, 2008. Elevation-Dependent Trends in Precipitation Observed during NAME. *Monthly Weather Review*, **136(12)**, 4962-4979.

Ruxton, G. D, 2006. The unequal variance *t*-test is an underscored alternative to Student's *t*-test and the Mann-Whitney *U* test. *Behavior Ecology*, 688-690.

Sampson, G. and E. Pytlak, 2008. Educating the public on the North American Monsoon System. National Weather Service, Tucson, Arizona. *National Oceanic and Atmospheric Administration*, 1-4.

Schrage, J. M., Augustyn, S., and A. H. Fink, 2007. Nocturnal stratiform cloudiness during the West African monsoon. *Meteorology and Atmospheric Physics,* **95**, 73-86.

Shaw, W. J., J. C. Doran, and R. L. Coulter, 2005. Boundary-layer evolution over Phoenix, Arizona and the premature mixing of pollutants in the early morning. *Atmospheric Environment*, **39**, 773-786.

Sheppard, P. R., A. C. Comrie, G. D. Packin, K. Angersbach, and M. K. Hughes, 2002. The climate of the US Southwest. *Climate Research*, **21**, 219-238.

Shi, C. N., H. J. S. Fernando, and P. Hyde, 2012. CMAQ predictions of tropospheric ozone in the US southwest: Influence of lateral boundary and synoptic conditions. *Science of the Total Environment*, **416**, 374-384.

Shutters S.T. and R. C. Balling, Jr., 2006. Weekly periodicity of environmental variables in Phoenix, Arizona. *Atmospheric Atmosphere* **40(2)**, 304–310.

Sugimoto, S., Sato, T. and K. Nakamura, 2013. Effects of synoptic-scale control on long-term declining trends of summer fog frequency over the Pacific side of the Hokkaido Island. *Journal of Applied Meteorology and Climatology,* **54**, 2226-2242.

Tang, M. and E. R. Reiter, 1984. Plateau monsoons of the Northern Hemisphere: A comparison between North America and Tibet. Monthly Weather Review, **112**, 617-637.

VanCuren, R., 2015. Transport aloft drives peak ozone in the Mojave Desert. *Atmospheric Environment*, **109**, 331-341.

Vasques, T., 2011. Weather Analysis & Forecasting. *Weather Graphics Technologies*, Garland, Texas, pp. 7.

Vogel, R. M, 1986. The Probability Plot Correlation Coefficient test for the normal, lognormal, and Gumbel distributional hypotheses. *Water Resources* Research, **22(4)**, 587-590.

U.S. Census, 2010: Arizona State and County Quick Facts. http://quickfacts.census.gov/qfd/states/04000.

U.S. Census Bureau, 2017. https://www.census.gov/library/publications.2015. February 13, 2018.

U.S. Census Bureau, 2018. https://www.census.gov/library/publications.2015. October 4, 2018.

U.S. Environmental Protection Agency (U.S. EPA), 2003. Guidelines for developing an air quality (ozone and $PM_{2.5}$) forecasting program. *United States Environmental Protection Agency*, EPA-456/R-03-002.

U.S. Environmental Protection Agency (U.S. EPA), 2018. https://www.epa.gov/outdoor-air-quality-data. August 1, 2018.

U.S. Environmental Protection Agency (EPA), 2017. https://www.epa.gov/outdoor-air-quality-data. February 19, 2018.

U.S. Environmental Protection Agency (U.S. EPA Ozone), 2018. https://www.epa.gov/sites/production/files/2015-10/documents/20151001_air_quality_index_updates.pdf. October 7, 2018.

Wayne, R. P., 1987. The photochemistry of ozone. *Atmospheric Environment*, **21**, 1683-1694.

Wallace, C. E., R. A. Maddox, and K. W. Howard. 1999. Summertime convective storm environments in central Arizona: Local observations. *Weather and Forecasting*, **14(6)**, 994-1006.

Watson, A. I., R. C. Holle, and R. E. Lopez, 1994. Cloud-to-ground lightning and upper-air patterns during bursts and breaks in the Southwest Monsoon. *Monthly Weather Review*, **122(8)**, 1726-1739.

Watson, A. I., R. E. Lopez, and R. L. Holle, 1994. Diurnal cloud-to-ground lightning patterns in Arizona during the Southwest Monsoon. *Monthly Weather Review*, **122(8)**, 1716-1725.

Wilks, D., 2011. Statistical Methods in the Atmospheric Sciences. *Elesevier Academic Press*, San Diego, California, pp. 519-562.

Yamasoe, M. A., B. Sauvage, V. Thouret, P. Nédélec, E. Le Flochmoen, and B. Barret, 2015. Analysis of tropospheric ozone and carbon monoxide profiles over South American based on MOZAIC/IAGOS database and model simulations. *Tellus B: Chemical and Physical Meteorology*, **67(1)**, 1-29.

Zehnder, J. A., L. Y. Zhang, D. Hansford, A. Radzan, N. Selover, and C. M. Brown, 2006. Using digital cloud photogrammetry to characterize the onset and transition from shallow to deep convection over orography. *Monthly Weather Review*, **134(9)**, 2527-2546.